JPET Fast Forward. Published on October 18, 2021 as DOI: 10.1124/jpet.121.000821
This article has not been copyedited and formatted. The final version may differ from this version.

CNS Distribution of an Opioid Agonist Combination with Synergistic Activity

Jessica I. Griffith*, Minjee Kim, Daniel J. Bruce, Cristina D. Peterson, Kelley F. Kitto, Afroz S. Mohammad, Sneha Rathi, Carolyn A. Fairbanks, George L. Wilcox, William F. Elmquist**

Brain Barriers Research Center (JIG, MK, AM, SR, WFE) Department of Pharmaceutics (JIG, MK, AM, SR, CAF, WFE) Department of Pharmacology (DJB, CAF, GLW) Department of Neuroscience (CDP, KFK, CAF, GLW), Department of Dermatology (GLW), University of Minnesota, Minneapolis

Elmquist Laboratory

*Corresponding author: Jessica I. Griffith, grif0285@umn.edu, (612) 625-2446, Department of Pharmaceutics, College of Pharmacy, University of Minnesota Twin Cities, 308 Harvard St SE, Minneapolis, MN 55455

**Secondary corresponding author: William F. Elmquist, elmqu011@umn.edu, (612) 625-0097, Department of Pharmaceutics, College of Pharmacy, University of Minnesota Twin Cities, 308 Harvard St SE, Minneapolis, MN 55455

JPET Fast Forward. Published on October 18, 2021 as DOI: 10.1124/jpet.121.000821
This article has not been copyedited and formatted. The final version may differ from this version.

Running title: **CNS Distribution of Opioid Agonist Combination**

Jessica I Griffith*, William F Elmquist**

*Corresponding author: grif0285@umn.edu, (612) 625-2446, Department of Pharmaceutics, College of Pharmacy, University of Minnesota Twin Cities, 308 Harvard St SE, Minneapolis, MN 55455

**Secondary corresponding author: elmqu011@umn.edu, (612) 625-0097, Department of Pharmaceutics, College of Pharmacy, University of Minnesota Twin Cities, 308 Harvard St SE, Minneapolis, MN 55455

Number of Pages: 28

Number of Tables: 6

Number of Figures: 8, 4 supplementary

Number of References: 36

Abstract: 249

Introduction: 683

Discussion: 1,420

Abbreviations:

AUC – Area under the concentration-time curve, BBB – Blood-brain barrier, BCRP – Breast cancer resistance protein, BKO – BCRP knockout, CDC – Centers for disease control and Prevention, CNS – Central Nervous system, DOR –δ-opioid receptor, Kp – overall tissue-to-plasma ratio or partition coefficient, Kp_t – tissue-to-plasma ratio at time t, Kp_{uu} - unbound partition coefficient, MOR – μ-opioid receptor, OMI – Oxymorphindole , P-gp – P-glycoprotein, PKO – P-glycoprotein knockout, TKO – Triple knockout

JPET Fast Forward. Published on October 18, 2021 as DOI: 10.1124/jpet.121.000821
This article has not been copyedited and formatted. The final version may differ from this version.

Recommended Section: Metabolism, Transport, and Pharmacogenomics

JPET Fast Forward. Published on October 18, 2021 as DOI: 10.1124/jpet.121.000821
This article has not been copyedited and formatted. The final version may differ from this version.

Abstract: Novel combinations of specific opioid agonists like loperamide and oxymorphindole targeting the μ- and δ-opioid receptors, respectively, have shown increased potency with minimized opioid-associated risks. However, whether their interaction is pharmacokinetic or pharmacodynamic in nature has not been determined. This study quantitatively determined whether these drugs have a pharmacokinetic interaction that alters systemic disposition or CNS distribution. We performed IV and oral *in vivo* pharmacokinetic assessments of both drugs following discrete dosing and administration in combination to determine whether the combination had any effect on systemic pharmacokinetic parameters or CNS exposure. Drugs were administered at 5 or 10 mg/kg IV or 30 mg/kg orally to ICR mice, and 5 mg/kg IV to FVB mice of the following genotypes: wild-type, *Bcrp*$^{-/-}$ (Bcrp knockout, BKO), *Mdr1a/b*$^{-/-}$ (P-gp knockout, PKO), and *Bcrp*$^{-/-}$ *Mdr1a/b*$^{-/-}$(triple knockout, TKO). In the combination, clearance of OMI was reduced by approximately half, and the plasma AUC increased. Consequently, brain and spinal cord AUCs for OMI in the combination also increased proportionately. Both loperamide and OMI are P-gp substrates, but administration of the two drugs in combination does not alter efflux transport at the CNS barriers. Because OMI alone shows appreciable brain penetration but little therapeutic efficacy on its own, and because loperamide's CNS distribution is unchanged in the combination, the mechanism of action for the increased potency of the combination is most likely pharmacodynamic, and most likely occurs at receptors in the peripheral nervous system. This combination has favorable characteristics for future development.

JPET Fast Forward. Published on October 18, 2021 as DOI: 10.1124/jpet.121.000821
This article has not been copyedited and formatted. The final version may differ from this version.

Significance Statement: Opioids have yet to be replaced as the most effective treatments for moderate-to-severe pain and chronic pain, but their side effects are dangerous. Combinations of opioids with peripheral activity, such as loperamide and oxymorphindole, would be valuable in that they are effective at much lower doses and have reduced risks for dangerous side effects, because the MOR-agonist is largely excluded from the CNS.

JPET Fast Forward. Published on October 18, 2021 as DOI: 10.1124/jpet.121.000821
This article has not been copyedited and formatted. The final version may differ from this version.

Introduction

Opioid agonists remain the most commonly prescribed treatment for moderate-to-severe pain, and have been in use for centuries (Presley and Lindsley, 2018a). The efficacy of these drugs in chronic and severe pain is well-characterized and has yet to be supplanted in modern clinical practice. However, along with their potent analgesic effects, opioid agonists are accompanied by well-known and sometimes dangerous adverse effects like constipation, sedation, respiratory depression, a liability to dependence, and the development of tolerance (Presley and Lindsley, 2018). In recent decades, rampant over prescription of opioids has led to an epidemic of opioid use disorder and overdose deaths. While subsequent enforcement efforts and prescribing guidance from the Centers for Disease Control and Prevention (CDC) hoped to stem the tide of overdose deaths (Dowell *et al.*, 2016), there are still few alternatives to opioid agonists when it comes to pain management. The CDC estimated in 2016 that approximately 20% of adults in the United States suffer from chronic pain (Dahlhamer *et al.*, 2018). A more recent study estimated that 4.8% of adults have high-impact chronic pain, and 13.8% experience pain that limits their daily activities (Pitcher *et al.*, 2019). This experience of pain can result in depression, anxiety, and poor overall quality of life. As a result, 3-4% of the entire US population is prescribed opiates for long-term pain management when the benefits of opioids are thought to outweigh the inherent risks (Dowell *et al.*, 2016). Individuals requiring long-term pain management may include cancer patients and those with postoperative pain, or individuals experiencing neuropathic and chronic pain from a variety of causes. In light of the risks of long-term opioid use, it is imperative that new, effective treatments with minimized risks become available for these patients.

In the search for novel treatments with reduced side effects, combinations of receptor-selective opioid agonists and other compounds have shown potential for potent analgesic and antihyperalgesic effects with reduced liability to tolerance and respiratory depression. Recently

JPET Fast Forward. Published on October 18, 2021 as DOI: 10.1124/jpet.121.000821
This article has not been copyedited and formatted. The final version may differ from this version.

published work from Bruce et al. showed that loperamide, a μ-opioid receptor (MOR) agonist, when dosed subcutaneously in a 1:1 combination with the δ-opioid receptor (DOR) agonist oxymorphindole (OMI), exhibited efficacious pain management in the face of inflammatory pain (Bruce *et al.*, 2019). This work is compelling in that efficacious pain management is achieved at many-fold lower doses of loperamide, and the combination is peripherally active (Bruce *et al.*, 2019; Uhelski *et al.*, 2020). There is a body of evidence supporting the hypothesis that heterodimerization of MORs with DORs results in downstream signaling that is different than conventional MOR dimerization (Gomes *et al.*, 2000, 2004; Lenard *et al.*, 2007; Schuster *et al.*, 2015). However, the potential for interactions in systemic disposition and CNS distribution that could contribute to the synergy of these two drugs has not been determined.

The distribution of opioids to the CNS plays a crucial role in the activity and use of opioid agonists. Sedation, respiratory depression, and addiction are mediated by MOR in the CNS as shown by studies in MOR knockout mice (Matthes *et al.*, 1996; Pattinson, 2008). Alterations in loperamide systemic pharmacokinetics or distribution to the CNS resulting from co-administration with OMI might play a role in the mechanism of action and safety of this combination. Because loperamide has long been known to be a P-glycoprotein (P-gp, ABCB1) substrate for efflux from the CNS as well as the gut (Schinkel *et al.*, 1996), it is possible that synergistic activity between these two drugs results from alterations in systemic pharmacokinetics or CNS drug distribution. This is especially important since the efflux status of OMI has not been determined. Therefore, two possible mechanisms exist that could explain this activity: a change in systemic pharmacokinetics and distribution to the CNS, or an interaction at the MOR/DOR receptor site (**Figure 1**).

In this study, we sought to clarify the nature of the interaction between loperamide and OMI by determining the effect on CNS distribution and systemic pharmacokinetics of the two drugs when administered alone and in combination. The primary objective of the current study

JPET Fast Forward. Published on October 18, 2021 as DOI: 10.1124/jpet.121.000821
This article has not been copyedited and formatted. The final version may differ from this version.

was to determine if the synergistic effect was related to changes in pharmacokinetics or changes in pharmacodynamics.

JPET Fast Forward. Published on October 18, 2021 as DOI: 10.1124/jpet.121.000821
This article has not been copyedited and formatted. The final version may differ from this version.

Materials and Methods

Reagents:

Loperamide hydrochloride and naltrindole hydrochloride were obtained from Tocris Bioscience (via Fisher Scientific). [^{6}H]Loperamide was purchased from Alsachim (Illkirch-Graffenstaden, France). Oxymorphindole (OMI), was a gift from the lab of Dr. Phil Portoghese (Portoghese *et al.*, 1988). All other chemical reagents were high-performance liquid chromatography grade and purchased from Thermo Fisher Scientific. Rapid equilibrium dialysis plates and inserts (8kDa molecular weight cutoff) were also purchased from Thermo Fisher Scientific.

Animals:

For the behavioral experiment, adult ICR-CD1 mice (22-29g, N = 90, male and female) were housed four (male) or five (female) to a cage and maintained on a 12-hour light/dark cycle with *ad libitum* access to water and food. Testing was performed during the light phase of this cycle. For the pharmacokinetic studies, male ICR mice (Charles River Laboratories) of age 8-14 weeks were used for initial studies as noted and housed in the Research Animal Resources (RAR) facility in the Academic Health Center of the University of Minnesota prior to use with. Subsequently, both male and female Friend Leukemia Virus strain B (FBV) mice of age 8-14 weeks of four different genotypes were used for transporter knockout studies. These genotypes included wild-type, *Bcrp*$^{-/-}$ (Bcrp knockout, BKO), *Mdr1a/b*$^{-/-}$ (P-gp knockout, PKO), and *Bcrp*$^{-/-}$ *Mdr1a/b*$^{-/-}$(triple knockout, TKO) mice (breeder pairs from Taconic Biosciences, Inc., Germantown, NY). Colonies of the FVB mice were maintained and housed in the RAR facility at the Academic Health Center of the University of Minnesota, and animal genotypes were regularly verified by tail snip (TransnetYX, Cordova, TN). All mice for pharmacokinetic studies were maintained on a 12-hour light/dark cycle with *ad libitum* access to water and food. Protocols for all animal experiments received approval by the University of Minnesota

JPET Fast Forward. Published on October 18, 2021 as DOI: 10.1124/jpet.121.000821
This article has not been copyedited and formatted. The final version may differ from this version.

Institutional Animal Care and Use Committee and were performed in accordance with the Guide for Care and Use of Laboratory Animals established by the U.S. National Institutes of Health.

Drug Preparation and Administration for Oral ED50 Calculation:

Formulations were prepared as a solution with 5% cremophore and DMSO, and subsequently diluted to administered concentrations with sterile water. Solutions were administered by oral gavage using a 20ga X 30mm sterile plastic feeding tube (Fine Science Tools, USA). No fluid was noted in the nose, an indication of aspirated solution, in any subject during or following gavage. Thermal nociceptive responses were assessed once prior to CFA administration, a baseline was assessed following CFA administration, and one hour following oral gavage of experimental compound.

Behavioral Measures:

The Hargreaves assay was used to assess peripheral thermal nociception, as described previously (Hargreaves *et al.*, 1988). Briefly, mice were placed in a small plastic box to restrict their movement on a heated glass floor (30°C). Animals were allowed to acclimate to the testing environment for 15 minutes prior to baseline withdrawal assessment. A radiant heat lamp was then shone on the left hind paw until the mouse withdrew the paw, and the paw latency was recorded (baseline) by a plantar stimulator antinociception meter (IITC Lifesciences, USA). A cutoff time of 20 s was established to prevent tissue damage. Three paw withdrawal latencies were recorded with a minimum of 30 s rest time between each test.

After determining naïve paw withdrawal latencies (PWLs), animals were briefly anesthetized using 2.5% isoflurane and 30 µL of an emulsion of 1:1 Complete Freund's Adjuvant (CFA) in saline was injected into the left hindpaw. 3-5 days following this injection, a well-characterized hyperalgesia was present in the left hindpaw, and post-CFA PWLs were assessed (post CFA value) (NEWBOULD, 1963). The experimental compounds (loperamide, OMI, or their

JPET Fast Forward. Published on October 18, 2021 as DOI: 10.1124/jpet.121.000821
This article has not been copyedited and formatted. The final version may differ from this version.

combination) were then delivered by oral gavage. One hour following oral gavage, thermal responses were again assessed (experimental value). Each animal received only one dose of compounds or of the combination. The experimenters were not blinded to drug or concentration during compound administration or behavioral testing. One experimenter delivered compound to all subjects, and a separate experimenter performed all PWL assessment.

Data Analysis of Behavioral Measures:

Thermal nociceptive responses following oral gavage of OMI, loperamide, or their combination were analyzed as a percentage of antihyperalgesia (%AH) given by the following equation:

$$\%\,\boldsymbol{AH} = \frac{([\boldsymbol{post\ CFA\ value - baseline}] - [\boldsymbol{experimental\ value - baseline}])}{(\boldsymbol{post\ CFA\ value - baseline}) \times \mathbf{100}} \quad (1)$$

The ED_{50} of loperamide and loperamide in the presence of oxymorphindole (Lo (+OMI)) were calculated using the graded dose-response curve method (Tallarida and Murray, 1987).

Systemic Pharmacokinetics and CNS Distribution Studies:

Single doses of loperamide, OMI, or a combination of the two drugs were administered to ICR mice via tail vain injection or oral gavage. Dosing formulations for both drugs were first prepared in sterile water for injection (SWFI) with 5% DMSO and 5% Cremophore. This solution was subsequently diluted 4X in SWFI to the final concentrations of 1 mg/mL for IV studies and 6 mg/mL for oral studies (1% DMSO, 1% Cremophore), with the exception of the first OMI IV study, which was diluted 2 mg/mL. The first OMI IV study was conducted with a dose of 10 mg/kg, which was well tolerated. However, when loperamide was initially dosed to two animals at 10 mg/kg IV, it was found to be poorly tolerated, and the dose was lowered to 5 mg/kg. All subsequent IV studies for both drugs were conducted with a dose of 5 mg/kg.

JPET Fast Forward. Published on October 18, 2021 as DOI: 10.1124/jpet.121.000821
This article has not been copyedited and formatted. The final version may differ from this version.

After IV administration, blood, brain, and spinal cord samples were collected at time points from 10 minutes to 16 hours (n=4 mice per time point). After oral administration, samples were collected from 30 minutes to 16 hours (n=4 mice per time point). Mice were euthanized via a CO_2 chamber. Blood was rapidly collected via cardiac puncture using heparinized syringes and transferred into heparinized tubes. Plasma was separated by centrifugation at 7500 rpm for 15 minutes at 4°C. Spinal cords were collected via the hydraulic extrusion method as described by Roberts et al. (Roberts *et al.*, 2005). Briefly, after decapitation, the spinal column rostral of the pelvis was removed. Then, a saline-filled syringe fixed with a blunt-tipped needle was inserted into the caudal end of the spinal column. The plunger was depressed to extrude the spinal column fully intact. Plasma, brain, and spinal cord were stored at -80°C until LC-MS/MS analysis. Prior to analysis, brain and spinal cord were thawed and homogenized in 2X (w/v) 5% BSA.

Transporter Knockout Pharmacokinetic and CNS Distribution Studies:

Systemic pharmacokinetic and CNS distribution studies to ascertain efflux transporter effects were conducted in FVB mice using IV administration as described above. Briefly, 5 mg/kg of loperamide, OMI, or the combination were administered via tail vein injection into wild-type, BKO, PKO, and TKO mice. Blood, brain, and spinal cord were harvested at time points ranging from 10 minutes to 16 hours (n=4 mice per time point, 2 male, 2 female) as described above. Samples were stored at -80°C until LC-MS/MS analysis. Prior to analysis, brain and spinal cord were thawed and homogenized in 2X (w/v) 5% BSA.

Rapid Equilibrium Dialysis (RED) for Free Fraction in Mouse Plasma and Brain Homogenate:

Free fractions of loperamide, OMI, and the combination in mouse plasma and brain homogenate were determined using RED devices according to the manufacturer's protocol

JPET Fast Forward. Published on October 18, 2021 as DOI: 10.1124/jpet.121.000821
This article has not been copyedited and formatted. The final version may differ from this version.

(Thermo Fisher). For brain homogenate, brain tissue was homogenized in 2 volumes (w/v) of PBS (pH 7.4) using a mechanical homogenizer. Both plasma and brain homogenate were spiked with loperamide, OMI, or a 1:1 combination to a final concentration of 5µM (for each drug) with 0.025% DMSO. Drug-matrix solutions (300µL) were then added to the sample chamber, and then 500µL of PBS (0.025% DMSO) was added to the buffer chamber. The plate was then sealed with adhesive film and incubated for 24 hours at 37°C in an orbital shaker set to 600 rpm. At 24 hours, samples were collected from both chambers and stored at -20°C until LC-MS/MS analysis. The undiluted free fraction (f_u) for both drugs was calculated with the following equation, as reported previously (Kalvass and Maurer, 2002).

$$f_u = \frac{1/D}{\left(\left(\frac{1}{f_{u,diluted}}\right) - 1\right) + 1/D} \qquad (2)$$

Where D is the dilution factor, or 3 as noted above.

LC-MS/MS Analysis:

Given their widely disparate hydrophobicity, separate LC-MS/MS methods were developed for loperamide and OMI. Both methods utilized reverse-phase liquid chromatography via an Aligent 1200 Series HPLC connected to a TSQ Quantum Classic mass spectrometer in positive ion mode. Briefly, both drugs and their internal standards were extracted from plasma, brain homogenate, and spinal cord samples via liquid-liquid extraction with 5X (v/v) ethyl acetate. Samples were vortexed for 5 minutes and centrifuged. Supernatant was collected and completely dried under nitrogen, and samples were reconstituted with mobile phase (MP). For loperamide, the internal standard was [^{6}H]-loperamide, and for OMI, the internal standard was

JPET Fast Forward. Published on October 18, 2021 as DOI: 10.1124/jpet.121.000821
This article has not been copyedited and formatted. The final version may differ from this version.

naltrindole. Both methods used a Phenomenex Synergi 4µm Polar-RP column (4µm, 75 x 2mm) for chromatographic separation and a MP flow rate of 0.3 mL/minute. For loperamide, the method was isocratic with a MP composition of aqueous phase (A) 45% distilled water with 0.1% formic acid and organic phase (B) of 55% acetonitrile with 0.1% formic acid and a total run time of 4 minutes. The OMI method utilized gradient elution with initial MP composition of aqueous phase (A) 75% distilled water with 0.1% formic acid and organic phase (B) 25% acetonitrile with 0.1% formic acid. The gradient was as follows: starting at 3 minutes, organic phase was increased to 90% over 0.75 minutes, held at 90% for 1.25 minutes, and decreased back to 25% over 0.5 minutes. It was then held at 25% for 4.5 minutes for a total runtime of 10 minutes. The *m/z* transition for all molecules were as follows: loperamide 478.1 → 267.3, [^{6}H]-loperamide 484.1 → 273.3, OMI 375.1 → 254.1, naltrindole 415.1 → 254.1. For both methods, the standard curve was linear over the range of 0.1-1000ng/mL (weighted $1/Y^2$) with coefficients of variation less than 15%. Data was acquired and analyzed using Xcalibur software. The inter-day variability for loperamide for all concentrations in the standard curve was less than 4%, the intra-day variability was less than 7%, and the limit of quantification was 0.1 ng/mL. For OMI, the inter-day variability was less than 15%, the intra-day variability was less than 7% and the limit of quantification was 0.1 ng/mL.

Pharmacokinetic Data Analysis

Plasma, brain, and spinal cord concentration-time profiles were analyzed using Phoenix WinNonlin version 8.3 (Certara USA Inc., Princeton, NJ). Brain concentrations were corrected for residual blood estimated at 1.4% of brain weight and with blood concentrations approximated by plasma concentrations (Fridén *et al.*, 2010). Pharmacokinetic parameters and metrics were calculated by performing noncompartmental analysis (NCA). Areas under the curve (AUCs) were determined by linear trapezoidal integration, where the AUC to the last time point (AUC_{Last}) was calculated directly. The AUC to time infinity ($AUC_{0\rightarrow\infty}$) was extrapolated from

JPET Fast Forward. Published on October 18, 2021 as DOI: 10.1124/jpet.121.000821
This article has not been copyedited and formatted. The final version may differ from this version.

the last time point to infinite time by dividing the concentration at the last time point (C_{Last}) by the terminal elimination rate constant (λ_z) as determined by the last 4 time points. In cases where the terminal slope was not sufficiently negative for the time course of these experiments, AUC_{Last} is reported rather than $AUC_{0\rightarrow\infty}$. Variances for $AUCs_{Last}$ were calculated using the Bailer method as reported in Phoenix WinNonlin (Bailer, 1988). Variances for $AUC_{0\rightarrow\infty}$ were calculated utilizing the Yuan extension of the Bailer method (Yuan, 1993).

Other pharmacokinetic parameters, including systemic clearance (CL), apparent clearance (CL/F), volume of distribution (V_{ss}) and apparent volume of distribution (V/F) as well as the terminal half-life ($t_{1/2}$) were also calculated by NCA in Phoenix software by the following methods:

$$\boldsymbol{CL\ and\ CL/F = \frac{Dose}{AUC_{0\rightarrow\infty}}} \qquad (3)$$

$$\boldsymbol{V_{ss} = MRT_{inf} \times CL} \qquad (4)$$

Where MRT_{inf} is the area under the first moment curve to infinity ($AUMC_{inf}$) divided by the $AUC_{0\rightarrow\infty}$.

$$\boldsymbol{t_{1/2} = \frac{ln\,(2)}{\lambda_z}} \qquad (5)$$

JPET Fast Forward. Published on October 18, 2021 as DOI: 10.1124/jpet.121.000821
This article has not been copyedited and formatted. The final version may differ from this version.

Where λ_z is the terminal first-order elimination rate constant associated with the log-linear portion of the concentration-time profile and is estimated by linear regression of time vs log-concentration.

The brain-to-plasma ratio, or brain tissue partition coefficient (Kp_{Brain}), for each drug was calculated as a ratio of the AUC of the brain concentration-time profile to the AUC of the plasma concentration-time profile (Equation 6). Similarly, the spinal cord-to-plasma ratio, or spinal cord tissue partition coefficient ($Kp_{Spinal\ Cord}$) was calculated as a ratio of the AUCs (Equation 7). The brain partition coefficient of free drug (Kp_{uu}) was calculated by multiplying the Kp_{Brain} by the ratio of unbound fractions in brain and plasma (Equation 8).

$$\boldsymbol{Kp_{Brain}} = \frac{\boldsymbol{AUC_{Brain}}}{\boldsymbol{AUC\ _{Plasma}}} \qquad (6)$$

$$\boldsymbol{Kp_{Spinal\ Cord}} = \frac{\boldsymbol{AUC_{Spinal\ Cord}}}{\boldsymbol{AUC_{Plasma}}} \qquad (7)$$

$$\boldsymbol{Kp_{uu}} = \boldsymbol{Kp_{Brain}} \times \frac{\boldsymbol{fu_{Brain}}}{\boldsymbol{fu_{Plasma}}} \qquad (8)$$

JPET Fast Forward. Published on October 18, 2021 as DOI: 10.1124/jpet.121.000821
This article has not been copyedited and formatted. The final version may differ from this version.

The tissue-to-plasma concentration ratio at time t is used to assess the extent of drug distribution over time, and will be notated as Kp_t values for both brain and spinal cord. These were calculated by the following:

$$\boldsymbol{Kp_t = \frac{Concentration_{tissue}}{Concentration_{plasma}}} \qquad (9)$$

The oral bioavailability (F) of both drugs was calculated by Equation 9:

$$\boldsymbol{F = \left\{\frac{[AUC_{(0\rightarrow\infty),plasma}]\ oral}{[AUC_{(0\rightarrow\infty),plasma}]IV}\right\}\left(\frac{Dose_{IV}}{Dose_{oral}}\right)} \qquad (10)$$

The distributional advantage (DA) achieved in mice lacking efflux transporters at the CNS barriers was calculated by the following equation.

$$\boldsymbol{DA_{(brain\ or\ spinal\ cord)} = \frac{Kp_{Brain\ or\ spinal\ cord}\ transporter\ knockout\ mice}{Kp_{Brain\ or\ spinal\ cord}\ wild-type\ mice}} \quad (11)$$

Statistical Analysis:

Data are represented as mean ± S.D. where applicable. For the behavioral study, the data were analyzed by non-linear regression, fitting an [agonist] vs. response curve to compare ED50 values by GraphPad Prism (version 8.4; Graphpad Software, La Jolla, CA), with a null

JPET Fast Forward. Published on October 18, 2021 as DOI: 10.1124/jpet.121.000821
This article has not been copyedited and formatted. The final version may differ from this version.

hypothesis that the ED50s for both data sets were equal. To compare AUCs among studies and between different tissues, a two-tailed unpaired *t* test was performed in Graphpad Prism with a null hypothesis that AUCs were equal. One-way ANOVA with Tukey's multiple comparisons test was performed to compare AUCs among WT and transporter knockout mice in Graphpad. A significance level of $P < 0.05$ was considered significant in all tests.

JPET Fast Forward. Published on October 18, 2021 as DOI: 10.1124/jpet.121.000821
This article has not been copyedited and formatted. The final version may differ from this version.

Results

Oral ED_{50} of Loperamide with and without OMI

The oral ED50 for loperamide was 51.8 mg/kg, and the oral ED50 for loperamide with OMI was 0.68 mg/kg. The best fit models for the dose-response curves resulted in a rejection of the null hypothesis ($p<0.01$), indicating that the potency of loperamide is increased when administered in combination with OMI. OMI individual ED50 could not be determined from these data.

Loperamide Disposition in ICR mice

In order to determine whether the co-administration of OMI and loperamide changes their CNS distribution or systemic pharmacokinetics, the two drugs were dosed alone and in combination. Brain, plasma, and spinal cord were collected and the concentrations of drug in each tissue were determined by LC-MS/MS. The total (bound + unbound drug) plasma, brain, and spinal cord concentration-time profiles for a single IV dose of loperamide alone (5 mg/kg) and loperamide in combination with OMI (5 mg/kg) in ICR mice are shown in Figures 3A and 3B. The plasma, brain, and spinal cord concentrations were below the limit of quantification for these studies at 12 and 16 hr time points, and therefore these were not included. Concentration-time profiles in all tissues exhibited biexponential decline over time. For loperamide alone, brain concentrations were significantly lower than that of plasma ($p < 0.001$), and spinal cord concentrations were lower than that of brain and significantly lower than plasma ($p < 0.001$) for the duration of the time course. For loperamide in combination with OMI, the same trend was observed. The tissue-to-plasma concentration ratios over time (Kp_{tBrain} and $Kp_{t\ Spinal\ Cord}$, Fig 3C and 3D) remain less than 1 for the duration of the time course. Accordingly, the overall Kp_{Brain} and $Kp_{Spinal\ Cord}$ as calculated by AUC ratios were also less than 1 for both discrete dosing and combination studies, which was expected, as loperamide is a P-gp substrate (Table 1).

JPET Fast Forward. Published on October 18, 2021 as DOI: 10.1124/jpet.121.000821
This article has not been copyedited and formatted. The final version may differ from this version.

Loperamide appears to reach a rapid distributional equilibrium in the CNS, as Kp_t did not change over the time course in either brain or spinal cord.

The pharmacokinetic parameters for loperamide alone and in combination with OMI are also listed in Table 1. There was no apparent difference among the parameters of $t_{1/2}$, CL, or V in the two studies. The difference among AUCs in plasma, brain, and spinal cord for loperamide alone and loperamide in combination with OMI was non-significant ($p = 0.966$, $p = 0.312$, and $p = 0.779$, respectively).

OMI disposition in ICR mice

The total (bound + unbound drug) plasma, brain, and spinal cord concentration-time profiles for single IV dose of OMI (10 mg/kg) and OMI in combination with loperamide (5 mg/kg) in ICR mice are shown in Figures 4A and 4B. The plasma, brain, and spinal cord concentrations show a pronounced distributional phase in both the discrete and combination studies. Brain and spinal cord concentrations are greater than plasma in the terminal phase for both studies, and this is apparent in Figure 4C, where Kp_{tBrain} (calculated as concentration ratios over time) is greater than unity at 2 hours for both OMI alone and OMI in combination. Similarly, in both the discrete dosing and combination studies, the $Kp_{tSpinal\ Cord}$ is greater than unity at 4 hours after administration (Figure 3D). OMI appears to take longer than loperamide to reach dynamic equilibrium between plasma and the CNS, as the Kp_t for both brain and spinal cord reaches a maximum around 8-12 hours after administration. The overall Kp_{Brain} was 2.0 for OMI dosed alone, and 1.4 for OMI dosed in combination (Table 1). The overall $Kp_{spinal\ Cord}$ was 0.51 in the discrete dosing study, and 0.42 in the combination study.

There was no difference in the half-life of OMI between the discrete and combination studies. In order to compare the AUCs between discrete dosing and the combination, dose-normalized AUCs were used, as the two studies were performed at difference doses. When dose-

JPET Fast Forward. Published on October 18, 2021 as DOI: 10.1124/jpet.121.000821
This article has not been copyedited and formatted. The final version may differ from this version.

normalized AUCs were compared, the plasma $AUCs_{0\rightarrow\infty}$ in the combination study (149 ± 16 h*ng/mL) was significantly higher than the plasma $AUC_{0\rightarrow\infty}$ for OMI alone (84 ± 6 h*ng/mL, $p < 0.001$, Table 1). There also appeared to be evidence of an increase in the dose-normalized AUC for both brain and spinal cord, though the difference was not statistically significant. For an additional comparison, the WT FVB studies for OMI alone and in combination with loperamide were used, as these studies were performed at the same dose. In WT FVB mice, the brain exposure of OMI was higher in combination with loperamide ($p = 0.0012$), however, the overall brain-to-plasma ratio was unchanged, indicating that the brain exposure increased in proportion to the plasma (Table 4).

Regarding OMI systemic exposure, because the AUC depends on dose and clearance, assuming linear pharmacokinetics, the most likely explanation for an increase in the AUC is a reduction in the systemic clearance of OMI. This is evident in a decreased clearance from 12 (L/h)/kg for OMI alone to 6.6 (L/h)/kg for OMI in combination (Table 1). Further evidence for linear pharmacokinetics and a reduction in systemic clearance can also be taken from the WT FVB studies, where the CL was nearly 10 (L/h)/kg for OMI alone, and 5 (L/h)/kg for OMI in combination (Table 4). Additionally, the systemic clearance is similar between the ICR mice (dosed at 10 mg/kg) and the WT FVB mice (dosed at 5mg/kg). Between those two studies, the AUCs were proportional, and the dose-normalized plasma AUCs for OMI IV in ICR and wild-type FVB are not significantly different ($p = 0.19$), indicating no significant strain differences.

Loperamide PO Systemic Pharmacokinetics and CNS distribution in ICR mice

Loperamide and OMI were also administered orally to assess systemic pharmacokinetics, CNS distribution, and bioavailability of the drugs when dosed in combination. The total plasma, brain, and spinal cord concentration-time profiles for loperamide in mice when dosed at 30mg/kg alone and in combination with OMI (30mg/kg) are shown in Figure 5A and 5B. Similarly to the IV studies, the brain and spinal cord concentrations in the PO study are less than the plasma for

JPET Fast Forward. Published on October 18, 2021 as DOI: 10.1124/jpet.121.000821
This article has not been copyedited and formatted. The final version may differ from this version.

the duration of the time course, and therefore the Kp_{tBrain} and $Kp_{tSpinal\ Cord}$ were also less than unity (Fig 5c and 5D). However, these concentration-time profiles in both studies show some evidence of multiple peaks, possibly because loperamide undergoes enterohepatic recycling (Miyazaki *et al.*, 1979). The t_{max} occurred at 1 hour for loperamide alone and at 4 hours for loperamide with OMI. The half-life for loperamide alone and in combination was 7 and 3.1 hours, respectively (Table 2). The apparent clearance (CL/F) for loperamide when dosed alone was similar to CL/F in the combination study, and the differences in the AUCs between the two studies for plasma, brain, and spinal cord were all nonsignificant (p=0.49, p=0.150, and p=0.720, respectively), and in accord with the IV studies, the bioavailability (F) was also not different (F=0.19 and F=0.25, Table 2).

OMI PO systemic Pharmacokinetics and CNS distribution in ICR mice

The total concentration-time profiles for OMI administered at 30 mg/kg alone and in combination are shown in Figure 6A and 6B. The t_{max} occurred at 1 hour for OMI alone and at 30 minutes for OMI in combination with loperamide. The Kp_{tBrain} for OMI alone and in combination showed a similar trend as in the IV studies, however the concentration in brain did not surpass the concentration in plasma until after 4 hours in the PO studies. The overall brain-to-plasma ratio for OMI was greater than 1 for both the discrete and combination studies, and were similar (Kp_{Brain} = 1.27 and 1.5, respectively, Table 2). In accordance to the IV studies, the concentrations of OMI in spinal cord were less than brain and only surpassed plasma concentrations at later time points. The overall spinal cord-to-plasma ratios were 0.54 for OMI alone and 0.82 in combination with loperamide (Table 2). The plasma AUC for OMI alone was significantly greater than AUC plasma for OMI in the combination (p=0.014). In accord with the IV studies, the oral bioavailability of OMI when dosed orally with loperamide was reduced from 0.55 to 0.17 (Table 2). However, when comparing the AUCs for brain and spinal cord for OMI

JPET Fast Forward. Published on October 18, 2021 as DOI: 10.1124/jpet.121.000821
This article has not been copyedited and formatted. The final version may differ from this version.

alone and OMI in combination, the AUCs were found to be not significantly different (p=0.111 and p=0.735, Table 2).

Loperamide disposition and CNS distribution in FVB knockout mice with and without OMI

To determine the contribution of P-gp and BCRP to the pharmacokinetics and CNS distribution of OMI and loperamide alone and in combination, 5mg/kg of both drugs and the combination were administered IV to wild-type (WT), BCRP knockout (BKO), P-gp knockout (PKO), and triple knockout (TKO) FVB mice. Concentration-time profiles for loperamide alone are shown in Supplementary Figure 1. Loperamide disposition in the wild-type mice when administered alone is similar to its disposition in the ICR mice, and the plasma AUCs for loperamide IV in ICR and wild-type FVB studies are not significantly different (p = 0.56), indicating no significant strain differences. The concentration-time profiles in the BKO mice also have similar kinetics and distribution to WT mice (Supplementary Fig. 1A and 1B), with brain and spinal concentrations lower than that of plasma. However, in the PKO and TKO mice, brain and spinal cord concentrations are higher than plasma for the duration of the time course. The terminal slopes for brain and spinal cord in these genotypes were not sufficiently negative to accurately extrapolate to time infinity, and therefore AUC_{Last} is reported for these tissues rather than $AUC_{0\rightarrow\infty}$. Upon comparison, the brain AUCs in the PKO and TKO mice were significantly higher than that of the WT mice ($p_{adj} < 0.001$, and $p_{adj} = 0.009$, respectively) as well as BKO mice ($p_{adj} <0.001$ and $p_{adj} =0.015$, respectively), but the brain AUCS in the PKO and TKO mice were not significantly different. The spinal cord AUCs in the PKO and TKO mice were also significantly higher than in the WT ($p_{adj} = 0.001$ and $p_{adj} = 0.003$, respectively) and the BKO mice ($p_{adj} = 0.001$ and $p_{adj} = 0.004$, respectively). This agrees with the prior characterization of loperamide as a P-gp substrate (Schinkel *et al.*, 1996). These data, for the first time, characterize the contribution of P-gp to efflux of loperamide from mouse spinal cord.

JPET Fast Forward. Published on October 18, 2021 as DOI: 10.1124/jpet.121.000821
This article has not been copyedited and formatted. The final version may differ from this version.

Additionally, the plasma terminal phase in both the PKO and TKO mice shows a reduced slope (Supplementary Fig 1C and 1D). When the plasma $AUC_{0\rightarrow\infty}$ was compared among the 4 genotypes, it was found that the WT AUC was not significantly different from the BKO mice (P_{adj} = 0.988) or the TKO mice (p_{adj} = 0.3151). However, the plasma AUC in PKO mice was significantly greater than in the WT mice (p_{adj} = 0.001), and the PKO and TKO mice were not significantly different (p_{adj} = 0.152). The systemic clearance appears to be reduced in mice lacking P-gp.

The concentration-time profiles and overall PK parameters for loperamide when administered with OMI show the same trends as the discrete dosing studies in all four genotypes (Sup. Fig 3A-D, Table 3). Again, the distribution of loperamide into the CNS is significantly increased in mice lacking P-gp. The half-life for loperamide also appears to be increased in mice lacking P-gp, and the clearance appears to be reduced. Similarly to the ICR mouse studies, the addition of OMI did not significantly alter the plasma, brain, or spinal cord AUCs in the WT FVB mice (Table 3, p = 0.914, p = 0.139, p = 0.617, respectively).

When the Kp_{tBrain} and $Kp_{tSpinal\ Cord}$ for loperamide alone are plotted over time, it is apparent that the mice with functional P-gp have similar tissue-to-plasma ratios (Fig. 7A and 7B). This is also reflected in the distributional advantage (DA) for loperamide in both brain (DA_{Brain}) and spinal cord ($DA_{Spinal\ Cord}$), which is around 2 in the BKO mice (Table 5). Alternatively, the mice lacking P-gp have much higher tissue-to-plasma ratios over time for both brain and spinal cord (Fig. 7A and 7B), with distributional advantages around and above 40 (Table 5). These same patterns are mirrored in the tissue-to-plasma ratios for loperamide in the combination study, where mice with functional P-gp have lower tissue-to-plasma ratios than the mice lacking P-gp (Fig 7C and 7D). Interestingly, the DA for brain and spinal cord may be reduced when loperamide is dosed in combination with OMI (Table 5).

JPET Fast Forward. Published on October 18, 2021 as DOI: 10.1124/jpet.121.000821
This article has not been copyedited and formatted. The final version may differ from this version.

OMI disposition and CNS distribution in FVB transporter knockout mice with and without loperamide

When OMI was administered alone in WT and BKO FVB mice, it showed similar distribution kinetics, with the brain and spinal cord concentrations surpassing that of plasma at the later time points (Supplementary Figure 2A and 2B). However, the PKO and TKO mice showed higher concentrations of OMI in brain and spinal cord throughout the time course. The terminal slopes for brain and spinal cord in these genotypes were not sufficiently negative to accurately extrapolate to time infinity, and therefore AUC_{Last} is reported for these tissues rather than $AUC_{0\rightarrow\infty}$. When the AUCs were compared, differences among brain and spinal cord AUCs in WT and BKO mice were not distinguishable ($p_{adj} = 0.551$ and $p_{adj} = 0.999$, respectively). The PKO and TKO mice, however, did have significantly higher AUCs than the WT mice and the BKO mice for both brain and spinal cord ($p_{adj} < 0.001$ for all cases). When the Kp_{tBrain} and $Kp_{tSpinal\ Cord}$ were compared over time, it was apparent that the mice with functional P-gp trend closely together at ratios near 1, lower than that of the PKO and TKO mice (Fig.8A-D). The DA_{Brain} for OMI in the knockouts was around 1 for the BKOs and 8 in the two genotypes lacking P-gp. The $DA_{Spinal\ Cord}$ was less than 1 in the BKOs and greater than 8 in the P-gp knockouts and triple knockouts (Table 5). All of these data indicate that OMI is a P-gp substrate but not a BCRP substrate.

For OMI discrete dosing, there was no difference in the plasma AUC or the half-life in any of the genotypes, implying that the systemic clearance and volume of distribution of OMI were not altered significantly by a lack of P-gp or BCRP (Table 4). The concentration-time profiles for OMI in combination with loperamide were similar to OMI alone for all 4 genotypes (Supplementary Figure 4). As observed in the ICR OMI IV studies, the clearance of OMI is reduced by approximately half when administered in combination with loperamide (Table 4), and as previously stated, the AUC_{Brain} for OMI in WT FVB mice is significantly higher when dosed in

JPET Fast Forward. Published on October 18, 2021 as DOI: 10.1124/jpet.121.000821
This article has not been copyedited and formatted. The final version may differ from this version.

combination with loperamide, but the overall Kp_{Brain} did not change. Also, as previously stated, the dose-normalized plasma AUCs for OMI IV in ICR and wild-type FVB are not significantly different ($p = 0.19$), indicating no significant strain differences. Interestingly, the reduction in clearance in the presence of loperamide that is observed in the ICR mice as well as the WT FVB mice is also consistent across all FVB genotypes when comparing OMI discrete dosing and the combination. This indicates that neither P-gp nor BCRP are likely to be involved in the mechanism of the interaction resulting in reduced systemic clearance of OMI.

Rapid Equilibrium Dialysis (RED) for Free Fraction in Mouse Plasma and Brain Homogenate

The free fraction in plasma and brain was determined by rapid equilibrium dialysis. The unbound brain partition coefficient (Kp_{uu}) was determined using the brain partition coefficients from wild-type FVB mouse studies as all of these studies were carried out at the same dose. The unbound fractions and Kp_{uu} are reported in Table 4. There was a significant increase in the unbound fraction of loperamide in plasma in the presence of OMI ($p<0.001$). However, there was no detectable difference in the unbound fraction of loperamide in brain homogenate with the presence of OMI. The fraction unbound of OMI was much higher than that of loperamide in both plasma and brain ($p<0.001$ in both cases), but there was no change in the unbound fraction of OMI in the presence of loperamide in either plasma ($p=0.165$) or in brain homogenate ($p=0.222$). The Kp_{uu} for both drugs was unchanged by the presence of the other. The Kp_{uu} for loperamide alone was 0.1 vs 0.11 in the presence of OMI, and the Kp_{uu} for OMI alone was 0.44 vs 0.42 in the presence of loperamide. This indicates that the brain penetration of both drugs is not significantly altered by a change in protein binding when they are administered in combination.

JPET Fast Forward. Published on October 18, 2021 as DOI: 10.1124/jpet.121.000821
This article has not been copyedited and formatted. The final version may differ from this version.

JPET Fast Forward. Published on October 18, 2021 as DOI: 10.1124/jpet.121.000821
This article has not been copyedited and formatted. The final version may differ from this version.

Discussion

Opioid agonists have a long history of effective use in the treatment of pain. However, along with their benefits come a number of caveats and risks like tolerance, dependence, and death (Presley and Lindsley, 2018b). This has led to demand for more prudent prescription practices and alternatives to the conventional use of opioids, and one promising avenue is through combinations of biased opioid agonists targeting the μ- and δ-opioid receptors. Loperamide is a MOR-agonist that is already FDA approved as an antidiarrheal medication, and oxymorphindole is a novel DOR-agonist with high specificity (Takemori *et al.*, 1992). In combination, these drugs have shown to be peripherally active with synergistic efficacy (Bruce *et al.*, 2019; Uhelski *et al.*, 2020) or at least significantly increased potency of loperamide, depending on the route of administration (Figure 2). While there are proposed mechanisms of action for this significant increase in potency, it could be due to a change in pharmacokinetics or CNS penetration (Figure 1). Our pharmacokinetic assessment sought to clarify whether these drugs have a pharmacokinetic interaction. In the present study, we administered loperamide and OMI alone and in combination to both wild-type ICR mice and four genotypes of FVB mice. The ICR mouse studies provide continuity with previously published pharmacodynamic studies and give information about the systemic disposition of both drugs, while the FVB mouse studies provide further insight into potential interactions of the two drugs at efflux transporters in the barriers of the CNS.

The results from the loperamide IV administration studies in ICR mice as well as WT FVB mice indicate that OMI has no significant effect on loperamide systemic pharmacokinetics or CNS distribution that might alter the activity or safety of this drug. With reference to safety, MOR agonists are of particular concern, as the reward signaling and adverse effects of dependence and respiratory depression are mediated by MORs in the CNS (Matthes *et al.*, 1996; Pattinson, 2008). The present studies show no change in the Kp_{Brain}, $Kp_{Spinal\ Cord}$ or the

JPET Fast Forward. Published on October 18, 2021 as DOI: 10.1124/jpet.121.000821
This article has not been copyedited and formatted. The final version may differ from this version.

unbound brain partition coefficient (Kp_{uu}), indicating that OMI has no effect on the CNS partitioning or active concentration of loperamide in the brain. This supports previous studies that show this combination has reduced liability for respiratory depression (a centrally-mediated adverse effect) compared to that of other, more brain-penetrant MOR-agonists (Bruce *et al.*, 2019). Following oral administration of the combination, there is no significant change in loperamide's systemic disposition, CNS distribution, or oral bioavailability. Given that the combination was administered at doses nearly 10-fold higher than the oral ED_{50} for this pharmacokinetic assessment, the likelihood of a pharmacokinetic interaction that changes the efficacy or safety of loperamide is even lower at the therapeutic oral doses, and would be of little concern for future development of this combination therapy.

In assessing the disposition and CNS distribution of OMI for the first time, it was found that OMI has appreciable CNS penetration, and that the plasma and CNS exposure of OMI is increased in the presence of loperamide. According to the IV administration studies in ICR and WT FVB mice, while the overall exposure in the CNS increases when OMI is administered with loperamide, the increase in CNS exposure is proportional to the increased plasma exposure. Additionally, the unbound fraction of OMI does not change in the presence of loperamide in either brain or plasma, and therefore the unbound partitioning of OMI into the brain is also unchanged. Further, given OMI's tolerability in ICR mice at a higher dose of 10 mg/kg IV, and the fact that DORs do not promote the undesirable effect respiratory depression, the distribution of OMI to the CNS is not a present concern with regards to safety. In fact, certain DORs have been shown to modulate some opioid effects such as tolerance; therefore OMI CNS penetration could be an advantage of the combination (Zhu *et al.*, 1999; Pradhan *et al.*, 2009).

For IV administration, the systemic exposure of OMI is increased in the presence of loperamide. The increase in the plasma AUC of OMI when co-administered with loperamide in both the ICR IV studies as well as the WT IV studies is due to the reduction in clearance

JPET Fast Forward. Published on October 18, 2021 as DOI: 10.1124/jpet.121.000821
This article has not been copyedited and formatted. The final version may differ from this version.

observed in the presence of loperamide. The metabolism and elimination of OMI have not been previously characterized, and therefore, we cannot speculate on a potential mechanism. However, given the fact that the reduction in clearance was observed in the combination studies in all four FVB genotypes, it is unlikely that either P-gp or BCRP play a role in this particular interaction. In the case of oral administration, the systemic exposure of OMI is significantly reduced. This is likely due to the decreased bioavailability of OMI when administered in the combination. According to the pharmacodynamic data, significantly lower oral doses of the combination show increased potency, and therefore a potential reduction in the bioavailability of OMI is not likely to be a limitation of the combination.

With regards to an interaction at the CNS barriers, a significant factor in many drugs' CNS distribution to the brain and spinal cord is efflux by ABC transporters. Loperamide has been previously characterized as a P-gp substrate (Schinkel *et al.*, 1996), but not a BCRP substrate, and how these transporters factor into loperamide's spinal cord distribution were unknown. Our studies show that loperamide is not a strong BCRP substrate, and that P-gp plays a significant role in excluding loperamide from spinal cord. Further, the substrate status of OMI has never been determined. The current study indicates that OMI is a substrate of P-gp, but not a substrate of BCRP. Additionally, because neither drug shows increased CNS tissue partitioning after co-administration in the studies described herein, there is no evidence that P-gp is saturated when the drugs are co-administered. A large body of research shows that efflux transport systems at the BBB are robust even in cases where the BBB is disrupted either by the presence of a tumor or by artificial means (Goutal *et al.*, 2018; de Gooijer *et al.*, 2021; Griffith *et al.*, 2021). While some studies have shown that the administration of loperamide with P-gp modulators and inhibitors like quinidine could pose the risk of classical opioid effects (Sadeque *et al.*, 2000), post-marketing assessments of loperamide when administered in combination with a variety of other P-gp substrates show that MOR-associated adverse effects are unlikely to

JPET Fast Forward. Published on October 18, 2021 as DOI: 10.1124/jpet.121.000821
This article has not been copyedited and formatted. The final version may differ from this version.

occur, implying that loperamide's access to the CNS is not enhanced to a therapeutically significant extent (Vandenbossche *et al.*, 2010).

While the CNS exposure of OMI may be increased after IV administration of the combination due to a reduction in its systemic clearance, given that the unbound CNS partitioning of both drugs is unchanged in the combination. Given the fact that the drugs appear to have no significant interaction at the CNS barriers, and the fact that OMI is not an efficacious analgesic agent on its own, the most likely mechanism for the interaction between loperamide and OMI is an alteration in pharmacodynamics at receptors in the peripheral nervous system. A large body of research has shown co-localization of MOR and DOR receptors and evidence of heterodimerization, especially in inflammatory pain states (Gomes *et al.*, 2004; Bruce *et al.*, 2019). Previous studies have shown that the synergy between specific MOR- and DOR-agonists requires protein kinase C epsilon (PKCε), and that DOR agonism is retained only in the case of biased signaling where specific agonists promote DOR and MOR phosphorylation but not DOR and MOR internalization (Pradhan *et al.*, 2009; Schuster *et al.*, 2015; Derouiche *et al.*, 2020). The mechanism of synergy for OMI and loperamide is therefore most likely that MORs and DORs form heteromers that remain localized at the cell membrane of primary afferents and retain PKCε-dependent signaling.

This conclusion regarding the peripherally-mediated activity of OMI and loperamide is another promising step in the development of peripherally-restricted opioids for the management of chronic and severe pain that significantly reduce the potential for tolerance, dependence, and overdose deaths. No peripherally-restricted opioids have been approved for the treatment of chronic pain, but their development is of increasing interest. A number of bi-specific agonists have been proposed, and previous work shows that bispecific agonists with a specific linker length have pronounced synergy and modulation of undesirable side effects (Daniels *et al.*, 2005; Lenard *et al.*, 2007; Ding *et al.*, 2018; Lei *et al.*, 2020). This strategy is

attractive for future drug development, and accounting for biased signaling of peripherally-restricted combinations of MOR and DOR agonists will likely lead to the development of safer and more effective analgesics.

Acknowledgements

The authors thank Phil Portoghese and Eyup Akgün for the generous gift of oxymorphindole for these experiments as well as James Fisher for assistance with LC-MS/MS method development and maintenance.

JPET Fast Forward. Published on October 18, 2021 as DOI: 10.1124/jpet.121.000821
This article has not been copyedited and formatted. The final version may differ from this version.

Authorship Contributions

Participated in Research Design: Elmquist, Wilcox, Fairbanks, Kim.

Conducted Experiments: Griffith, Kim, Bruce, Peterson, Kitto, Mohammad, Rathi.

Performed Data Analysis: Griffith, Kim, Bruce.

Wrote or Contributed to the writing of the manuscript: Griffith, Bruce, Peterson, Kitto

JPET Fast Forward. Published on October 18, 2021 as DOI: 10.1124/jpet.121.000821
This article has not been copyedited and formatted. The final version may differ from this version.

References

Bailer AJ (1988) Testing for the equality of area under the curves when using destructive measurement techniques. *J Pharmacokinet Biopharm*, doi: 10.1007/BF01062139.

Bruce DJ, Peterson CD, Kitto KF, Akgün E, Lazzaroni S, Portoghese PS, Fairbanks CA, and Wilcox GL (2019) Combination of a δ-opioid Receptor Agonist and Loperamide Produces Peripherally-mediated Analgesic Synergy in Mice. *Anesthesiology*, doi: 10.1097/ALN.0000000000002840.

Dahlhamer J, Lucas J, Zelaya, C, Nahin R, Mackey S, DeBar L, Kerns R, Von Korff M, Porter L, and Helmick C (2018) Prevalence of Chronic Pain and High-Impact Chronic Pain Among Adults — United States, 2016. *MMWR Morb Mortal Wkly Rep*, doi: 10.15585/mmwr.mm6736a2.

Daniels DJ, Lenard NR, Etienne CL, Law PY, Roerig SC, and Portoghese PS (2005) Opioid-induced tolerance and dependence in mice is modulated by the distance between pharmacophores in a bivalent ligand series. *Proc Natl Acad Sci U S A*, doi: 10.1073/pnas.0506627102.

de Gooijer MC, Kemper EM, Buil LCM, Çitirikkaya CH, Buckle T, Beijnen JH, and van Tellingen O (2021) ATP-binding cassette transporters restrict drug delivery and efficacy against brain tumors even when blood-brain barrier integrity is lost. *Cell Reports Med*, doi: 10.1016/j.xcrm.2020.100184.

Derouiche L, Pierre F, Doridot S, Ory S, and Massotte D (2020) Heteromerization of endogenous mu and delta opioid receptors induces ligand-selective co-targeting to lysosomes. *Molecules*, doi: 10.3390/molecules25194493.

Ding H, Kiguchi N, Yasuda D, Daga PR, Polgar WE, Lu JJ, Czoty PW, Kishioka S, Zaveri NT,

and Ko MC (2018) A bifunctional nociceptin and mu opioid receptor agonist is analgesic without opioid side effects in nonhuman primates. *Sci Transl Med*, doi: 10.1126/scitranslmed.aar3483.

Dowell D, Haegerich TM, and Chou R (2016) CDC guideline for prescribing opioids for chronic pain-United States, 2016. *JAMA - J Am Med Assoc*, doi: 10.1001/jama.2016.1464.

Fridén M, Ljungqvist H, Middleton B, Bredberg U, and Hammarlund-Udenaes M (2010) Improved measurement of drug exposure in the brain using drug-specific correction for residual blood. *J Cereb Blood Flow Metab*, doi: 10.1038/jcbfm.2009.200.

Gomes I, Gupta A, Filipovska J, Szeto HH, Pintar JE, and Devi LA (2004) A role for heterodimerization of μ and δ opiate receptors in enhancing morphine analgesia. *Proc Natl Acad Sci U S A*, doi: 10.1073/pnas.0307601101.

Gomes I, Jordan BA, Gupta A, Trapaidze N, Nagy V, and Devi LA (2000) Heterodimerization of mu and delta opioid receptors: A role in opiate synergy. *J Neurosci*, doi: 10.1523/jneurosci.20-22-j0007.2000.

Goutal S, Gerstenmayer M, Auvity S, Caillé F, Mériaux S, Buvat I, Larrat B, and Tournier N (2018) Physical blood-brain barrier disruption induced by focused ultrasound does not overcome the transporter-mediated efflux of erlotinib. *J Control Release*, doi: 10.1016/j.jconrel.2018.11.009.

Griffith JI, Sarkaria JN, and Elmquist WF (2021) Efflux Limits Tumor Drug Delivery Despite Disrupted BBB.

Hargreaves K, Dubner R, Brown F, Flores C, and Joris J (1988) A new and sensitive method for measuring thermal nociception in cutaneous hyperalgesia. *Pain*, doi: 10.1016/0304-3959(88)90026-7.

Kalvass JC, and Maurer TS (2002) Influence of nonspecific brain and plasma binding on CNS exposure: Implications for rational drug discovery. *Biopharm Drug Dispos*, doi: 10.1002/bdd.325.

Lei W, Vekariya RH, Ananthan S, and Streicher JM (2020) A Novel Mu-Delta Opioid Agonist Demonstrates Enhanced Efficacy With Reduced Tolerance and Dependence in Mouse Neuropathic Pain Models. *J Pain*, doi: 10.1016/j.jpain.2019.05.017.

Lenard NR, Daniels DJ, Portoghese PS, and Roerig SC (2007) Absence of conditioned place preference or reinstatement with bivalent ligands containing mu-opioid receptor agonist and delta-opioid receptor antagonist pharmacophores. *Eur J Pharmacol*, doi: 10.1016/j.ejphar.2007.02.040.

Lötsch J, Stockmann A, Kobal G, Brune K, Waibel R, Schmidt N, and Geisslinger G (1996) Pharmacokinetics of morphine and its glucuronides after intravenous infusion of morphine and morphine-6-glucuronide in healthy volunteers. *Clin Pharmacol Ther*, doi: 10.1016/S0009-9236(96)90058-2.

Matthes HWD, Maldonado R, Simonin F, Valverde O, Slowe S, Kitchen I, Befort K, Dierich A, Le Meur M, Dolie P, Tzavara E, Hanoune J, Roques BP, and Kieffer BL (1996) Loss of morphine-induced analgesia, reward effect and withdrawal symptoms in mice lacking the μ-opioid-receptor gene. *Nature*, doi: 10.1038/383819a0.

Miyazaki H, Nambu K, Matsunaga Y, and Hashimoto M (1979) Disposition and metabolism of [14C]loperamide in rats. *Eur J Drug Metab Pharmacokinet*, doi: 10.1007/BF03189427.

NEWBOULD BB (1963) CHEMOTHERAPY OF ARTHRITIS INDUCED IN RATS BY MYCOBACTERIAL ADJUVANT. *Br J Pharmacol Chemother*, doi: 10.1111/j.1476-5381.1963.tb01508.x.

Pattinson KTS (2008) Opioids and the control of respiration.

Pitcher MH, Von Korff M, Bushnell MC, and Porter L (2019) Prevalence and Profile of High-Impact Chronic Pain in the United States. *J Pain*, doi: 10.1016/j.jpain.2018.07.006.

Portoghese PS, Sultana M, Nagase H, and Takemori AE (1988) Application of the message-address concept in the design of highly potent and selective non-peptide .delta. opioid receptor antagonists. *J Med Chem*, doi: 10.1021/jm00397a001.

Pradhan AAA, Becker JAJ, Scherrer G, Tryoen-Toth P, Filliol D, Matifas A, Massotte D, Gavériaux-Ruff C, and Kieffer BL (2009) In vivo delta opioid receptor internalization controls behavioral effects of agonists. *PLoS One*, doi: 10.1371/journal.pone.0005425.

Presley CC, and Lindsley CW (2018a) DARK Classics in Chemical Neuroscience: Opium, a Historical Perspective. *ACS Chem Neurosci*, doi: 10.1021/acschemneuro.8b00459.

Presley CC, and Lindsley CW (2018b) DARK Classics in Chemical Neuroscience: Opium, a Historical Perspective. *ACS Chem Neurosci* **9**.

Roberts JC, Grocholski BM, Kitto KF, and Fairbanks CA (2005) Pharmacodynamic and pharmacokinetic studies of agmatine after spinal administration in the mouse. *J Pharmacol Exp Ther*, doi: 10.1124/jpet.105.086173.

Sadeque AJM, Wandel C, He H, Shah S, and Wood AJJ (2000) Increased drug delivery to the brain by P-glycoprotein inhibition. *Clin Pharmacol Ther*, doi: 10.1067/mcp.2000.109156.

Schinkel AH, Wagenaar E, Mol CAAM, and Van Deemter L (1996) P-glycoprotein in the blood-brain barrier of mice influences the brain penetration and pharmacological activity of many drugs. *J Clin Invest*, doi: 10.1172/JCI118699.

Schuster DJ, Metcalf MD, Kitto KF, Messing RO, Fairbanks CA, and Wilcox GL (2015) Ligand requirements for involvement of PKCε in synergistic analgesic interactions between spinal

μ and δ opioid receptors. *Br J Pharmacol*, doi: 10.1111/bph.12774.

Takemori AE, Sultana M, Nagase H, and Portoghese PS (1992) Agonist and antagonist activities of ligands derived from naltrexone and oxymorphone. *Life Sci* **50**.

Tallarida RJ, and Murray RB (1987) Graded dose—response, in *Manual of Pharmacologic Calculations* p.

Uhelski ML, Bruce D, Speltz R, Wilcox GL, and Simone DA (2020) Topical Application of Loperamide/Oxymorphindole, Mu and Delta Opioid Receptor Agonists, Reduces Sensitization of C-fiber Nociceptors that Possess NaV1.8. *Neuroscience*, doi: 10.1016/j.neuroscience.2020.08.022.

Vandenbossche J, Huisman M, Xu Y, Sanderson-Bongiovanni D, and Soons P (2010) Loperamide and P-glycoprotein inhibition: assessment of the clinical relevance. *J Pharm Pharmacol*, doi: 10.1211/jpp.62.04.0001.

Yoshida K, Nambu K, Arakawa S, Miyazaki H, and Hashimoto M (1979) Metabolites of loperamide in rats. *Biol Mass Spectrom*, doi: 10.1002/bms.1200060606.

Yuan J (1993) Estimation of variance for AUC in animal studies. *J Pharm Sci*, doi: 10.1002/jps.2600820718.

Zhu Y, King MA, Schuller AGP, Nitsche JF, Reidl M, Elde RP, Unterwald E, Pasternak GW, and Pintar JE (1999) Retention of supraspinal delta-like analgesia and loss of morphine tolerance in δ opioid receptor knockout mice. *Neuron*, doi: 10.1016/S0896-6273(00)80836-3.

JPET Fast Forward. Published on October 18, 2021 as DOI: 10.1124/jpet.121.000821
This article has not been copyedited and formatted. The final version may differ from this version.

Footnotes

This work was supported by The University of Minnesota PharmacoNeuroImmunology Training Grant, T32 DA007097–32, supported DJB. NIDA R01 DA 015438–10 to G.L.W. supported initial studies. We also acknowledge preclinical development grants from the University of Minnesota Committee on Pharmaceutical Development (CPD) and MN-REACH Program (to GLW). GLW holds the R.W. Goltz Professorship in Dermatology, which also provided support.

Dr. Bruce, Dr. Fairbanks, and Dr. Wilcox have an international patent application published under the publication number WO 2017/165558 A1. The other authors declare no conflicts of interest.

Reprint requests should be sent to William F Elmquist, elmqu011@umn.edu, University of Minnesota College of Pharmacy, Department of Pharmaceutics, 9-177 Weaver Densford Hall, 308 Harvard St. Se, Minneapolis, MN 55455

JPET Fast Forward. Published on October 18, 2021 as DOI: 10.1124/jpet.121.000821
This article has not been copyedited and formatted. The final version may differ from this version.

Figure Legends

Figure 1. Previous publications have shown synergistic activity of loperamide and OMI when co-administered. Two possible mechanisms exist for this synergy: a change in CNS distribution and/or systemic disposition, and heterodimerization of MORs and DORs that result in altered downstream signaling.

Figure 2. Potency of oral loperamide with and without co-administration with OMI in ICR mice. Peripherally-mediated thermal nociceptive responses in the Hargreaves assay were assessed. Following CFA-induced inflammation in the hindpaw, subjects were given an oral gavage of loperamide, OMI or combination and post-drug nociceptive responses were taken one hour post-administration. Responses are reported as % anti-hyperalgesia, which was used to generate dose-response curves. The data were analyzed by non-linear regression, fitting an [agonist] vs. response curve to compare ED50 values by GraphPad Prism 8.4.

Figure 3. Loperamide IV Pharmacokinetics and CNS Distribution in ICR mice. (A) Plasma, brain, and spinal cord concentration-time profiles following a single IV dose (5 mg/kg) of loperamide (B) Plasma, brain, and spinal cord concentration-time profiles following a single IV dose of loperamide (5 mg/kg) co-administered with OMI (5 mg/kg) (C) Kp_{tBrain} of loperamide from the pharmacokinetic studies described by A and B (D) $Kp_{tSpinal\ Cord}$ from the pharmacokinetic studies described by A and B

Figure 4. OMI IV Pharmacokinetics and CNS Distribution in ICR mice. (A) Plasma, brain, and spinal cord concentration-time profiles following a single IV dose (10 mg/kg) of OMI (B) Plasma, brain, and spinal cord concentration-time profiles following a single IV dose of OMI (5 mg/kg) co-administered with loperamide (5 mg/kg) (C) Kp_{tBrain} of OMI from the pharmacokinetic studies described by A and B (D) $Kp_{tSpinal\ Cord}$ of OMI from the pharmacokinetic studies described by A and B

JPET Fast Forward. Published on October 18, 2021 as DOI: 10.1124/jpet.121.000821
This article has not been copyedited and formatted. The final version may differ from this version.

Figure 5. Loperamide Oral Pharmacokinetics and CNS Distribution in ICR mice. (A) Plasma, brain, and spinal cord concentration-time profiles following a single oral dose (30 mg/kg) of loperamide (B) Plasma, brain, and spinal cord concentration-time profiles following a single oral dose of loperamide (30 mg/kg) co-administered with OMI (30 mg/kg) (C) Kp_{tBrain} of loperamide from the pharmacokinetic studies described by A and B (D) $Kp_{tSpinal\ Cord}$ from the pharmacokinetic studies described by A and B

Figure 6. OMI Oral Pharmacokinetics and CNS Distribution in ICR mice. (A) Plasma, brain, and spinal cord concentration-time profiles following a single oral dose (30 mg/kg) of OMI (B) Plasma, brain, and spinal cord concentration-time profiles following a single IV dose of OMI (30 mg/kg) co-administered with loperamide (30 mg/kg) (C) Kp_{tBrain} of OMI from the pharmacokinetic studies described by A and B (D) $Kp_{tSpinal\ Cord}$ of OMI from the pharmacokinetic studies described by A and B

Figure 7. Loperamide CNS Distribution in FVB Transporter Knockout mice. (A) Kp_{tBrain} of loperamide in WT, BKO, PKO and TKO FVB mice (B) $Kp_{tSpinal\ Cord}$ of loperamide in WT, BKO, PKO and TKO FVB mice (C) Kp_{tBrain} of loperamide when co-administered with OMI in WT, BKO, PKO and TKO FVB mice (D) $Kp_{tSpinal\ Cord}$ of loperamide when co-administered with OMI in WT, BKO, PKO and TKO FVB mice

Figure 8. OMI CNS Distribution in FVB Transporter Knockout mice. (A) Kp_{tBrain} of OMI in WT, BKO, PKO and TKO FVB mice (B) $Kp_{tSpinal\ Cord}$ of OMI in WT, BKO, PKO and TKO FVB mice (C) Kp_{tBrain} of OMI when co-administered with loperamide in WT, BKO, PKO and TKO FVB mice (D) $Kp_{tSpinal\ Cord}$ of OMI when co-administered with loperamide in WT, BKO, PKO and TKO FVB mice

JPET Fast Forward. Published on October 18, 2021 as DOI: 10.1124/jpet.121.000821
This article has not been copyedited and formatted. The final version may differ from this version.

Table 1. Summary pharmacokinetic parameters for loperamide and OMI in ICR mice following IV administration alone and in combination. OMI exposures are dose-normalized. A two-tailed unpaired t-test was performed to compare AUCs among tissues (see results) and between the same tissues in discrete vs. combination studies (*p <0.001)

Results are presented as mean or mean ± S.D.

Parameter	Loperamide Alone (5mg/kg)	Loperamide in Combination (5mg/kg)	OMI Alone (dose-normalized)	OMI in Combination (dose-normalized)
$t_{1/2}$ (h)	1.16	1.23	3.35	3.9
CL (L/h)/kg	3.6	3.6	12	6.6
V L/kg	4.7	4.9	17.6	11.6
$AUC_{0\rightarrow\infty}$ Plasma (h*ng)/mL	1389 ± 140	1374 ± 299	84 ± 6*	149 ± 16*
$AUC_{0\rightarrow\infty}$ Brain (h*ng)/g	257 ± 55	347 ± 65	175 ± 15	219 ± 20
$AUC_{0\rightarrow\infty}$ Spinal Cord (h*ng)/g	163 ± 32	151 ± 28	43 ± 3	63 ± 10
Kp_{Brain}	0.19	0.25	2.0	1.4
$Kp_{Spinal\ Cord}$	0.12	0.11	0.51	0.42

JPET Fast Forward. Published on October 18, 2021 as DOI: 10.1124/jpet.121.000821
This article has not been copyedited and formatted. The final version may differ from this version.

Table 2. Summary pharmacokinetic parameters for loperamide and OMI in ICR mice following oral administration alone and in combination. A two-tailed unpaired t-test was performed to compare AUCs among tissues (see results) and between the same tissues in discrete vs. combination studies (*p=0.014).

Results are presented as mean or mean ± S.D.

Parameter	Loperamide Alone (30 mg/kg)	Loperamide in Combination (30mg/kg)	OMI Alone (30 mg/kg)	OMI in Combination (30 mg/kg)
$t_{1/2}$ (h)	7	3.1	2.5	4.5
CL/F (L/h)/kg	19	15.5	22.3	51.2
V/F L/kg	192	70.3	80 L/kg	162
C_{max} (ng/mL)	235	370	345	186
T_{max} (h)	0.5	4	1	0.5
$AUC_{0\rightarrow\infty}$ Plasma (h*ng)/mL	1577 ± 427	1936 ± 290	1386 ± 191*	745 ± 166*
$AUC_{0\rightarrow\infty}$ Brain (h*ng)/g	94 ± 13	162 ± 40	1762 ± 296	1121 ± 262
$AUC_{0\rightarrow\infty}$ Spinal Cord (h*ng)/g	304 ± 220	223 ± 44	744 ± 273	615 ± 262
Kp_{Brain}	0.06	0.08	1.27	1.5
$Kp_{Spinal\ Cord}$	0.19	0.12	0.54	0.82
F	0.19	0.25	0.55	0.17

JPET Fast Forward. Published on October 18, 2021 as DOI: 10.1124/jpet.121.000821
This article has not been copyedited and formatted. The final version may differ from this version.

Table 3. Summary pharmacokinetic parameters of loperamide in WT, BKO, PKO, and TKO FVB mice following a single IV dose (5 mg/kg) and following co-administration with OMI (5 mg/kg). A two-tailed unpaired t-test was performed to compare AUCs among tissues within the same study (see results) and between the same tissues in discrete vs. combination studies. A one-way ANOVA with Tukey's multiple comparisons test was used to compare AUCs for the same tissue among different genotypes

Results are presented as mean or mean ± S.D.

Drug	Parameter	Wild-type	BKO	PKO	TKO
Loperamide alone	$t_{1/2}$ (h)	1.85	1.7	7.8	5.6
	CL (L/h)/kg	2.9	2.6	1.2	1.8
	V (L/kg)	6.6	7.0	10.6	10.1
	$AUC_{0\rightarrow\infty}$ or (last) Plasma (h*ng)/mL	1,686 ± 413	1,909 ± 312	4,302 ± 781	2,838 ± 273
	$AUC_{0\rightarrow\infty}$ or (last) Brain (h*ng)/g	173 ± 78	397 ± 105	17,503 ± 5,100	13,832 ± 3,503
	$AUC_{0\rightarrow\infty}$ or (last) Spinal Cord (h*ng)/g	70 ± 25	82 ± 9.6	8,752 ± 1,978	7,823 ± 2,403
	Kp_{Brain}	0.10	0.21	4.1	4.9
	$Kp_{Spinal\ cord}$	0.05	0.11	2.0	2.7
Loperamide in Combination	$t_{1/2}$ (h)	2.05	2.4	4.17	9.54
	CL (L/h)/kg	2.9	2.4	0.98	1.02
	V (L/kg)	6.9	5.67	4.46	13.2
	$AUC_{0\rightarrow\infty}$ or (last) Plasma (h*ng)/mL	1,744 ± 333	2,080 ± 207	5,266 ± 923	4,860 ± 1,377

JPET Fast Forward. Published on October 18, 2021 as DOI: 10.1124/jpet.121.000821
This article has not been copyedited and formatted. The final version may differ from this version.

	$AUC_{0\rightarrow\infty}$ or (last) Brain (h*ng)/g	460 ± 188	216 ± 27	13,350 ± 2,012	14,566 ± 2,713
	$AUC_{0\rightarrow\infty}$ or (last) Spinal Cord (h*ng)/g	90.2 ± 31.3	137 ± 26	10,516 ± 1,966	9,185 ± 1,400
	Kp_{Brain}	0.26	0.10	2.5	3.0
	$Kp_{Spinal\ cord}$	0.05	0.07	2.0	1.89

JPET Fast Forward. Published on October 18, 2021 as DOI: 10.1124/jpet.121.000821
This article has not been copyedited and formatted. The final version may differ from this version.

Table 4. Summary pharmacokinetic parameters determined by noncompartmental analysis of total drug concentrations of OMI in WT, BKO, PKO, and TKO FVB mice following a single IV dose (5 mg/kg) and following co-administration with loperamide (5 mg/kg). A two-tailed unpaired t-test was performed to compare AUCs among tissues within the same study (see results) and between the same tissues in discrete vs. combination studies. A one-way ANOVA with Tukey's multiple comparisons test was used to compare AUCs for the same tissue among different genotypes

Results are presented as mean or mean ± S.D.

Drug	Parameter	Wild-type	BKO	PKO	TKO
OMI alone	$t_{1/2}$ (h)	2.9	2.9	2.6	2.8
	CL (L/h)/kg	9.8	8.0	6.7	7.4
	V (L/kg)	24.9	16.6	15.5	15.5
	$AUC_{0\rightarrow\infty}$ or (last) Plasma (h*ng)/mL	508 ± 57	623 ± 86	735 ± 43	670 ± 42
	$AUC_{0\rightarrow\infty}$ or (last) Brain (h*ng)/g	500 ± 116	760 ± 66	5976 ± 184	5665 ± 159
	$AUC_{0\rightarrow\infty}$ or (last) Spinal Cord (h*ng)/g	172 ± 16	121 ± 27	5689 ± 607	2952 ± 62
	Kp_{Brain}	1.0	1.2	8.1	8.4
	$Kp_{Spinal\ cord}$	0.34	0.18	7.6	4.3
OMI in Combination	$t_{1/2}$ (h)	2.5	2.6	3.48	3.37
	CL (L/h)/kg	5.0	3.0	1.8	2.6
	V (L/kg)	13	8.7	5.8	10.1
	$AUC_{0\rightarrow\infty}$ or (last) Plasma (h*ng)/mL	1002 ± 167	1541 ± 245	2613 ± 258	1893 ± 130

JPET Fast Forward. Published on October 18, 2021 as DOI: 10.1124/jpet.121.000821
This article has not been copyedited and formatted. The final version may differ from this version.

$AUC_{0\rightarrow\infty}$ or (last) Brain (h*ng)/g	1115 ± 136	1076 ± 77	6993 ± 581	7128 ± 458
$AUC_{0\rightarrow\infty}$ or (last) Spinal Cord (h*ng)/g	326 ± 71	248 ± 32	3584 ± 260	3913 ± 203
Kp_{Brain}	1.1	0.71	2.7	3.7
$Kp_{Spinal\ cord}$	0.33	0.16	1.37	2.0

JPET Fast Forward. Published on October 18, 2021 as DOI: 10.1124/jpet.121.000821
This article has not been copyedited and formatted. The final version may differ from this version.

Table 5. Distributional advantage for brain and spinal cord in the 3 genotypes of transporter knockout FVB mice (BKO, PKO, and TKO mice). Determined by a ratio of Kps in each tissue to the corresponding Kp in wild-type FVB mice.

Genotype	Tissue	Loperamide alone	Lop in Combination	OMI alone	OMI in Combination
BKO	DA_{Brain}	2.1	0.38	1.2	0.71
	$DA_{Spinal\ Cord}$	2.2	1.4	0.53	0.53
PKO	DA_{Brain}	41	9.6	8.1	2.5
	$DA_{Spinal\ Cord}$	40	40	25	3.9
TKO	DA_{Brain}	49	11	8.4	3.4
	$DA_{Spinal\ Cord}$	54	38	14	6

JPET Fast Forward. Published on October 18, 2021 as DOI: 10.1124/jpet.121.000821
This article has not been copyedited and formatted. The final version may differ from this version.

Table 6. Unbound fractions of loperamide and OMI in brain and plasma determined from in vitro RED experiment after 24 incubation in 5 replicates. Unbound partition coefficients determined using data from WT FVB mice.

Results are presented as mean ± S.D.

Drug	Plasma fu (mean ± S.D.)	Brain fu (mean ± S.D.)	Kpuu (wild-type FVB mice)
Loperamide	0.0183 ± 0.0011*	0.0154 ± 0.0022	0.10
Loperamide (w/OMI)	0.0357 ± 0.0053*	0.0140 ± 0. 0016	0.11
OMI	0.192 ± 0.0754	0.0841 ± 0.0142	0.44
OMI (w/loperamide)	0.253 ± 0.0482	0.0951 ± 0.0187	0.42

JPET Fast Forward. Published on October 18, 2021 as DOI: 10.1124/jpet.121.000821
This article has not been copyedited and formatted. The final version may differ from this version.

Figure 1 and Visual Abstract

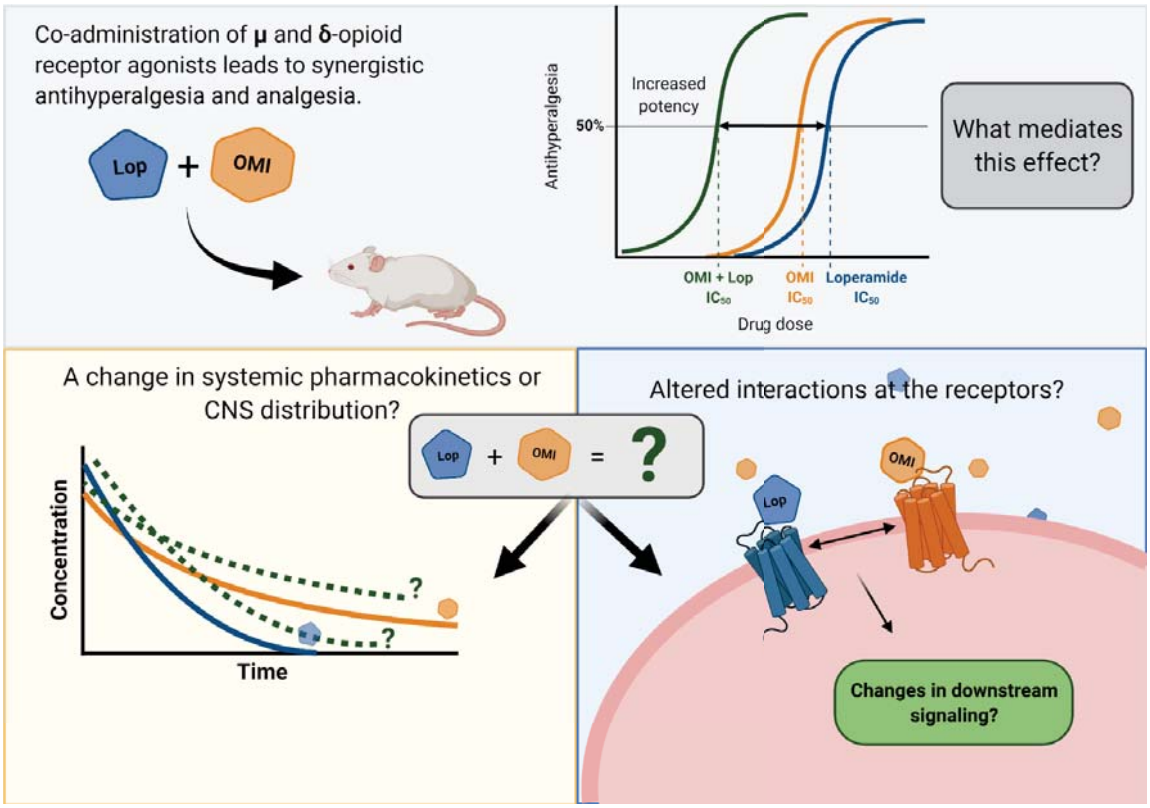

Figure 2

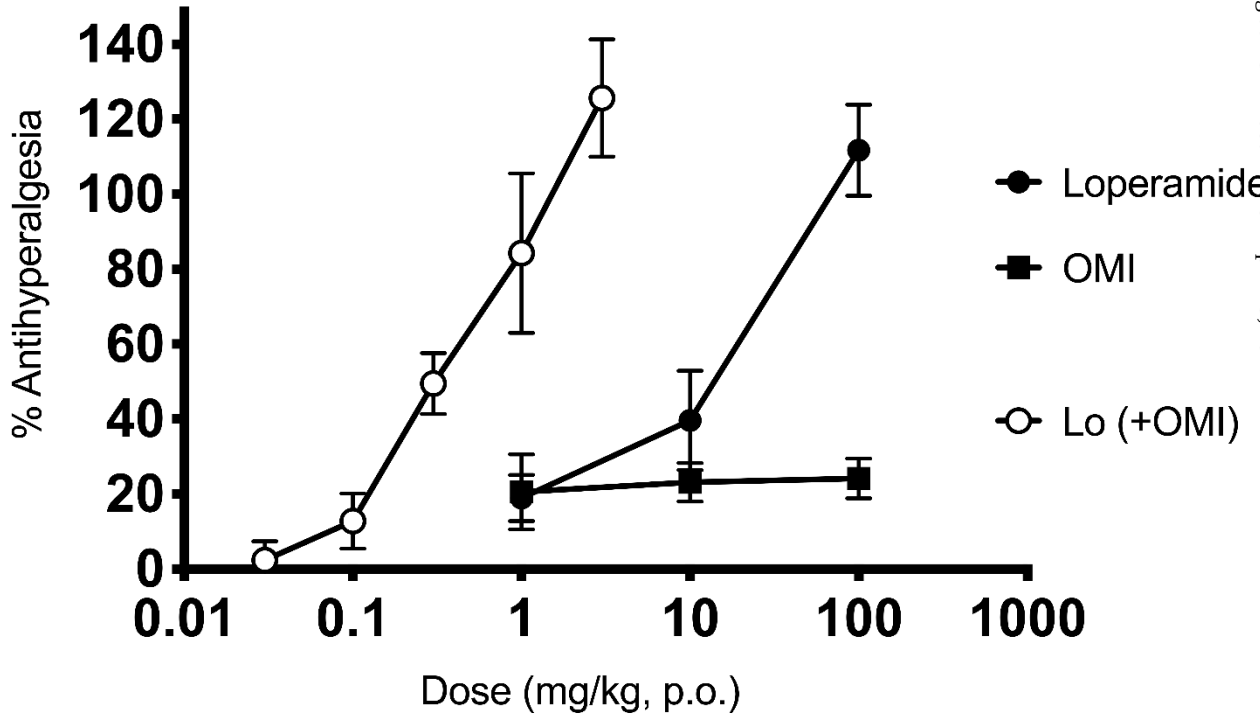

Figure 3

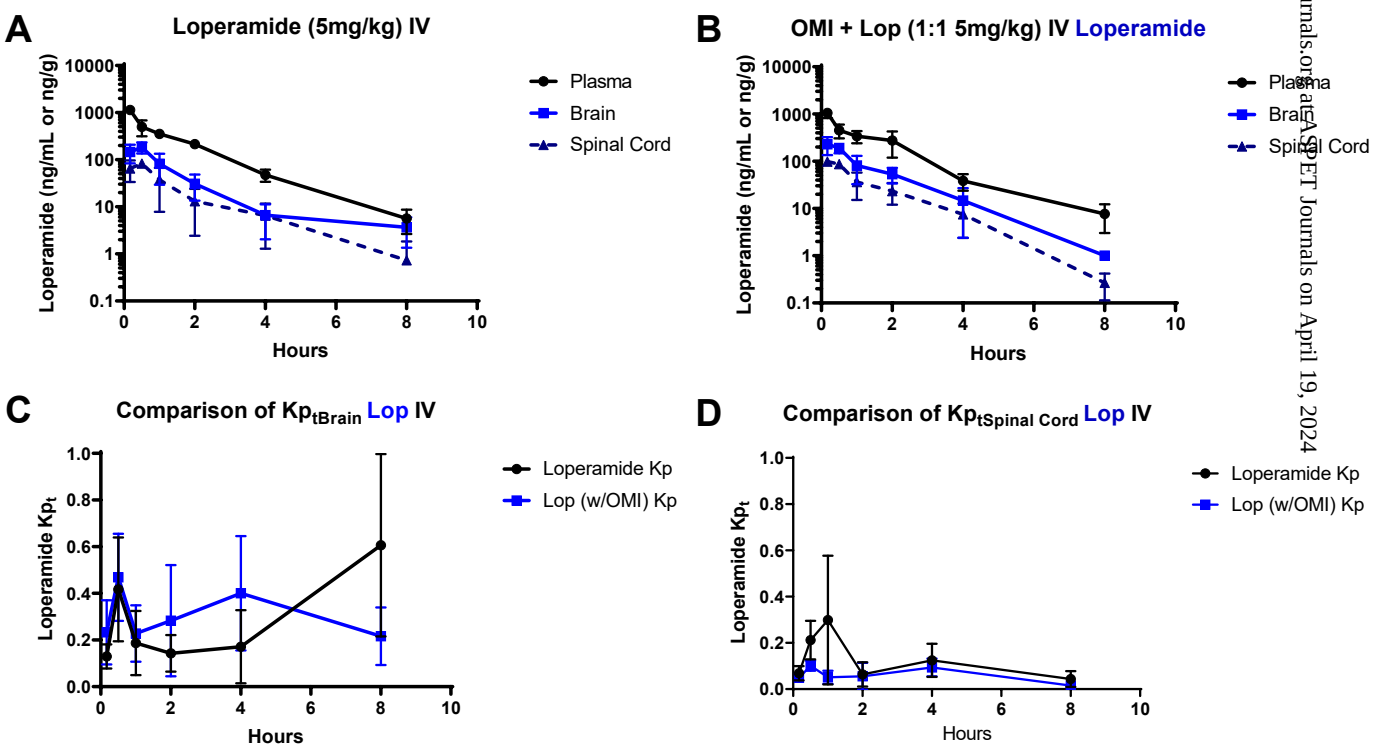

JPET Fast Forward. Published on October 18, 2021 as DOI: 10.1124/jpet.121.000821
This article has not been copyedited and formatted. The final version may differ from this version.

Figure 4

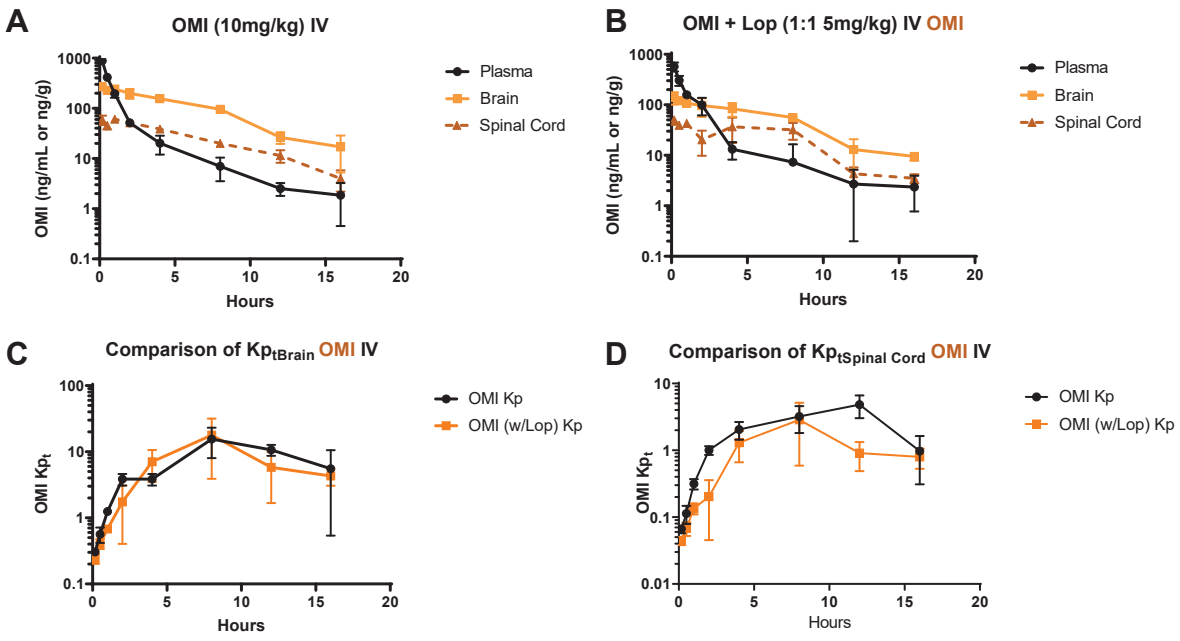

Figure 5

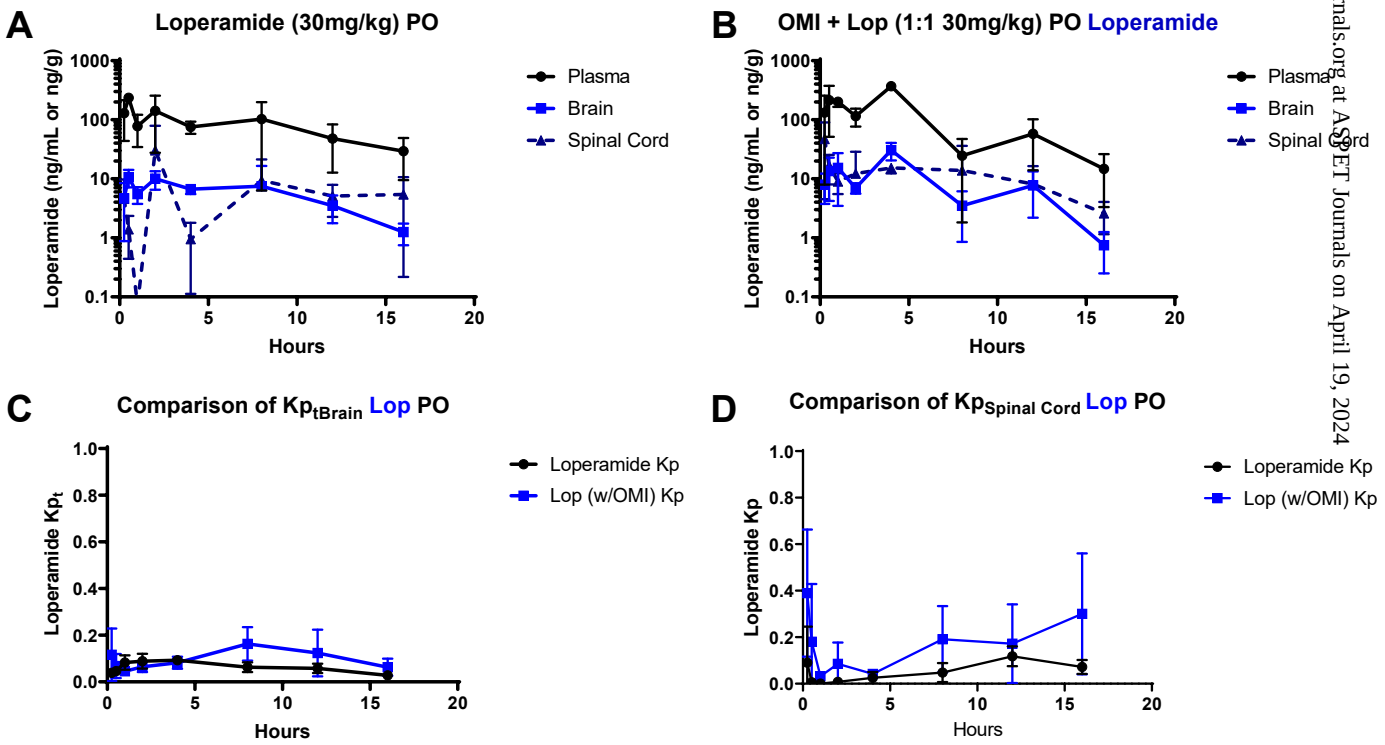

JPET Fast Forward. Published on October 18, 2021 as DOI: 10.1124/jpet.121.000821
This article has not been copyedited and formatted. The final version may differ from this version.

Figure 6

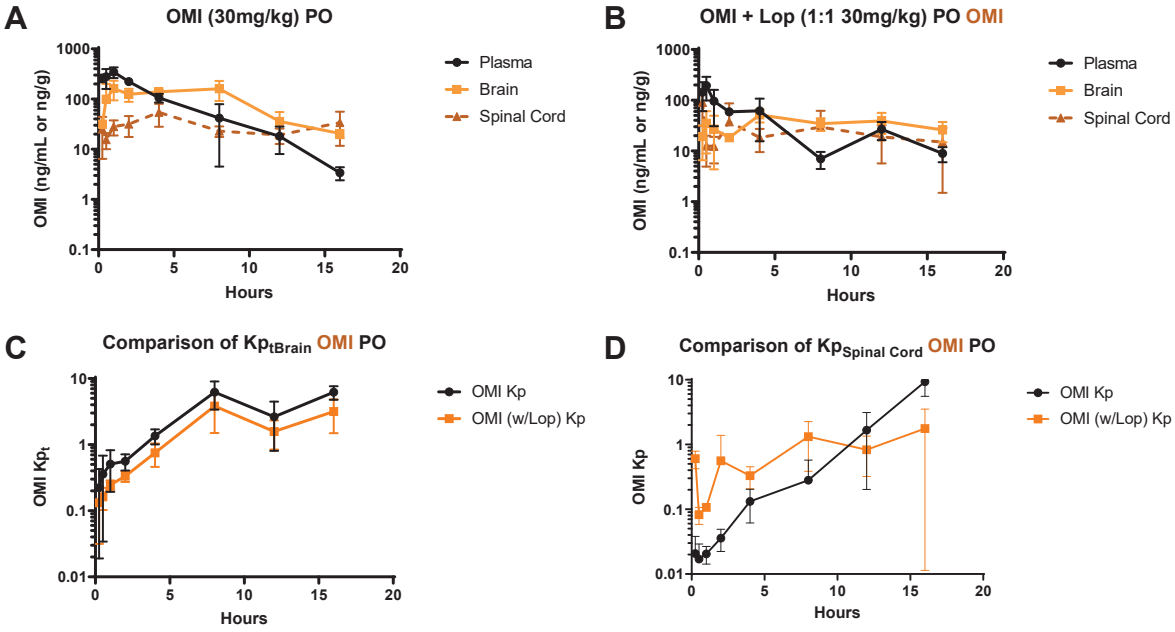

JPET Fast Forward. Published on October 18, 2021 as DOI: 10.1124/jpet.121.000821
This article has not been copyedited and formatted. The final version may differ from this version.

Figure 7

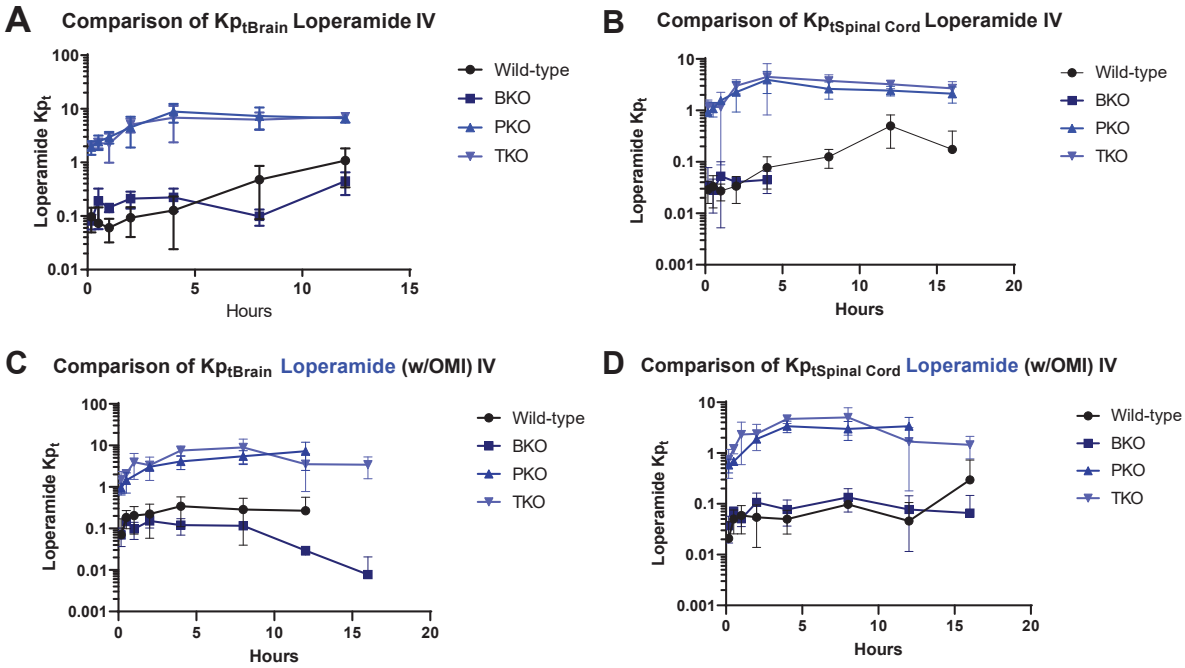

JPET Fast Forward. Published on October 18, 2021 as DOI: 10.1124/jpet.121.000821
This article has not been copyedited and formatted. The final version may differ from this version.

Figure 8

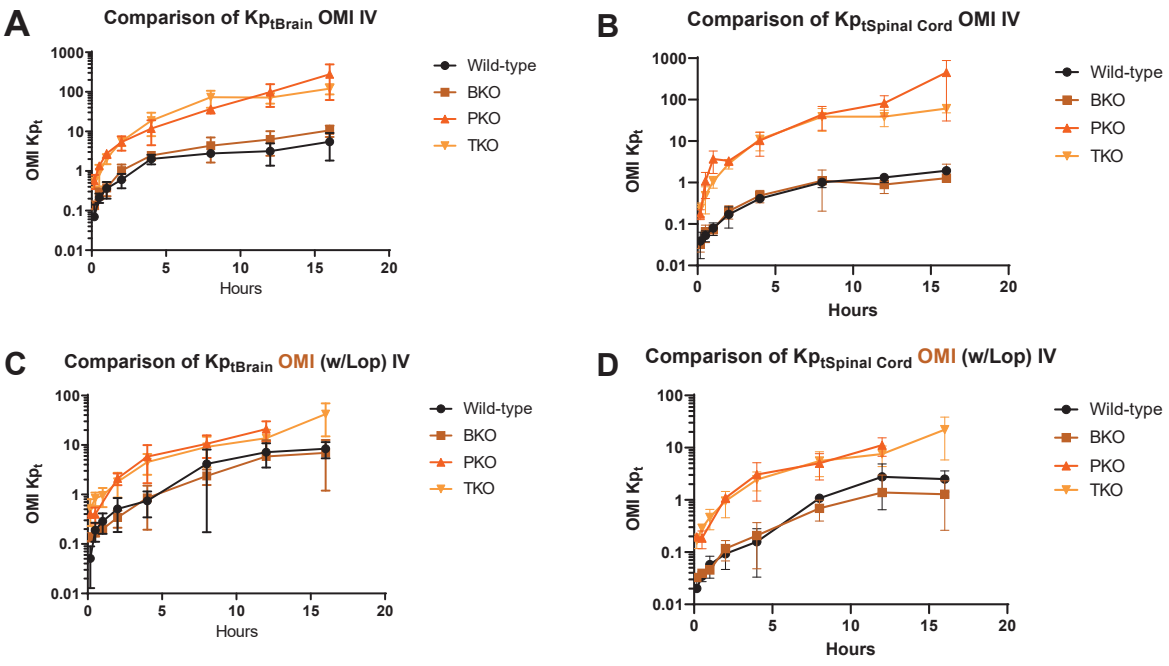

Journal of Pharmacology and Experimental Therapeutics

Manuscript Number: JPET-AR-2021-000821

Supplementary Figures

CNS Distribution of an Opioid Agonist Combination with Synergistic Activity

Jessica I. Griffith*, Minjee Kim, Daniel J. Bruce, Cristina D. Peterson, Kelley F. Kitto, Afroz S. Mohammad, Sneha Rathi, Carolyn A. Fairbanks, George L. Wilcox, William F. Elmquist**

Brain Barriers Research Center (JIG, MK, AM, SR, WFE) Department of Pharmaceutics (JIG, MK, AM SR, CAF, WFE) Department of Pharmacology (DJB, CAF, GLW) Department of Neuroscience (CDP, KFK, CAF, GW) University of Minnesota, Minneapolis

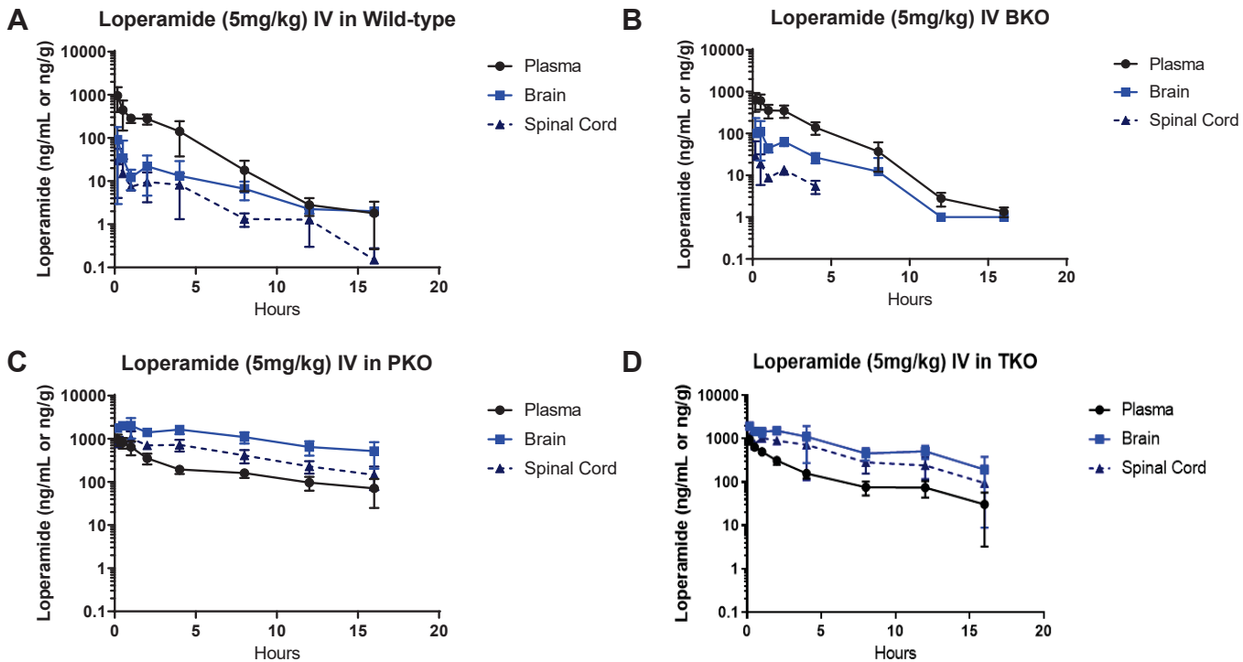

Supplementary Figure 1. Loperamide IV Pharmacokinetics and CNS Distribution in FVB mice. Plasma, brain, and spinal cord concentration-time profiles following a single IV dose of loperamide (5mg/kg) in (A) wild-type, (B) BCRP knockout, (C) P-gp knockout, and (D) triple knockout FVB mice

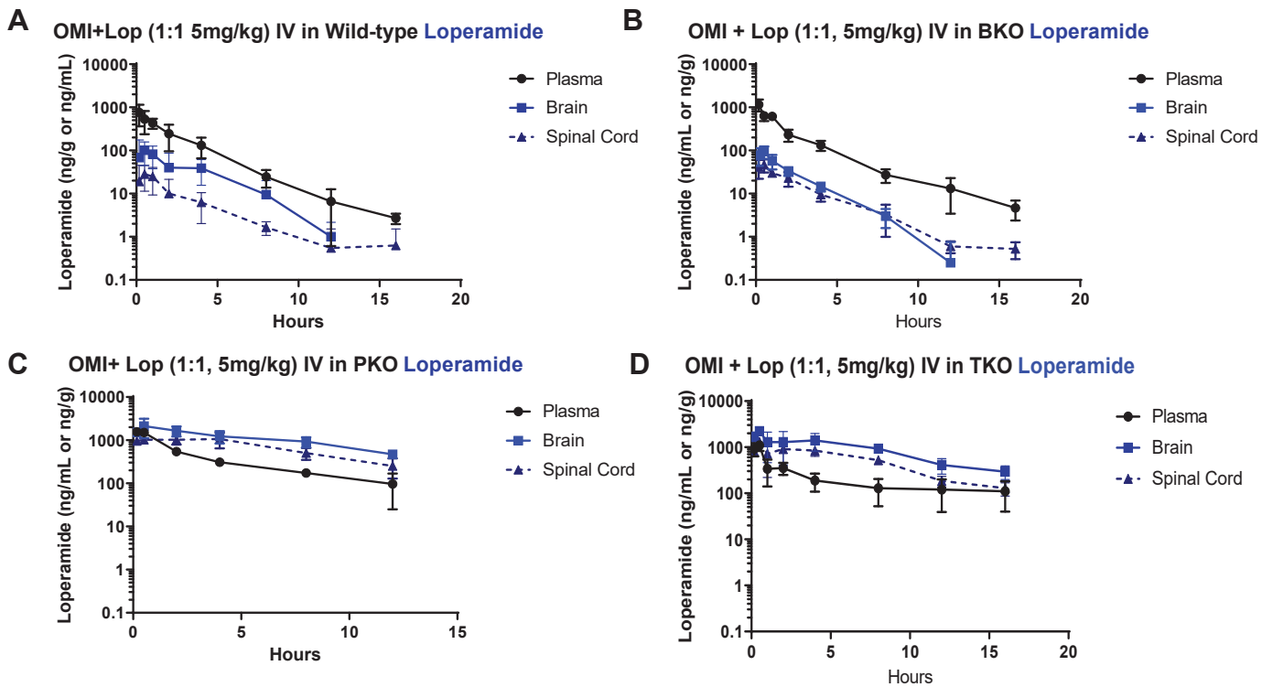

Supplementary Figure 2. Loperamide IV Pharmacokinetics and CNS distribution when Co-administered with OMI. Plasma, brain, and spinal cord concentration-time profiles following a single IV dose of loperamide (5mg/kg) co-administered with OMI (5mg/kg) in (A) Wild-type, (B) BCRP knockout, (C) P-gp knockout, and (D) triple knockout FVB mice

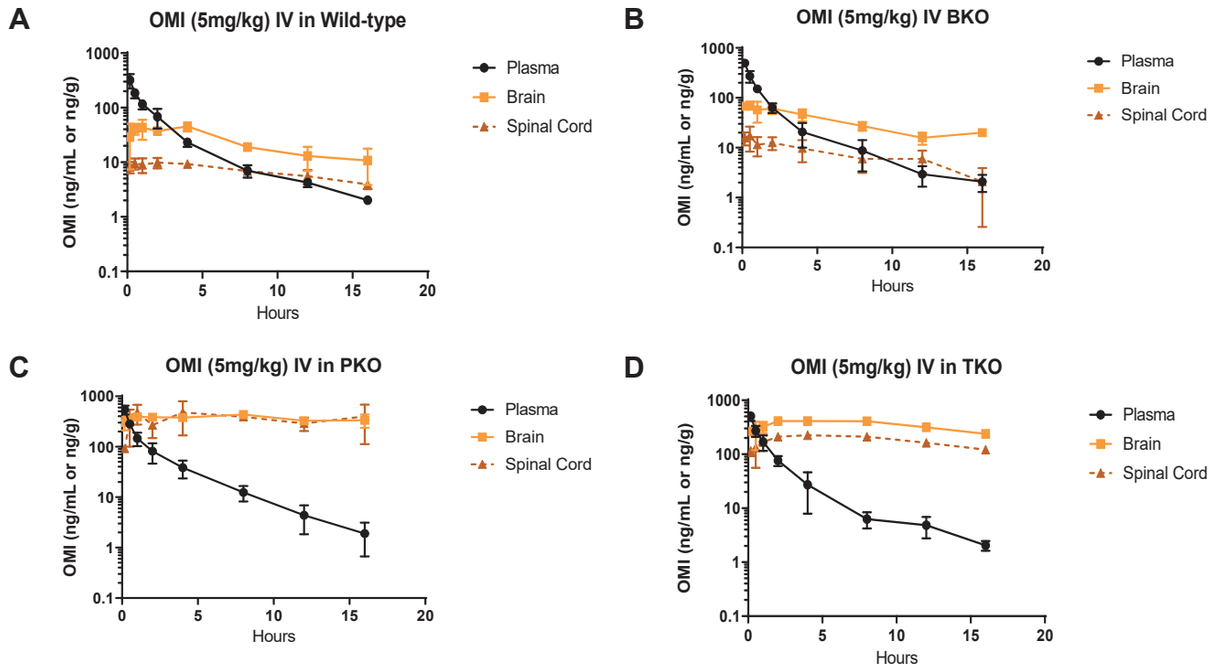

Supplementary Figure 3. OMI IV Pharmacokinetics and CNS Distribution in FVB mice. Plasma, brain, and spinal cord concentration-time profiles following a single IV dose of OMI (5mg/kg) in (A) wild-type, (B) BCRP knockout, (C) P-gp knockout, and (D) triple knockout FVB mice

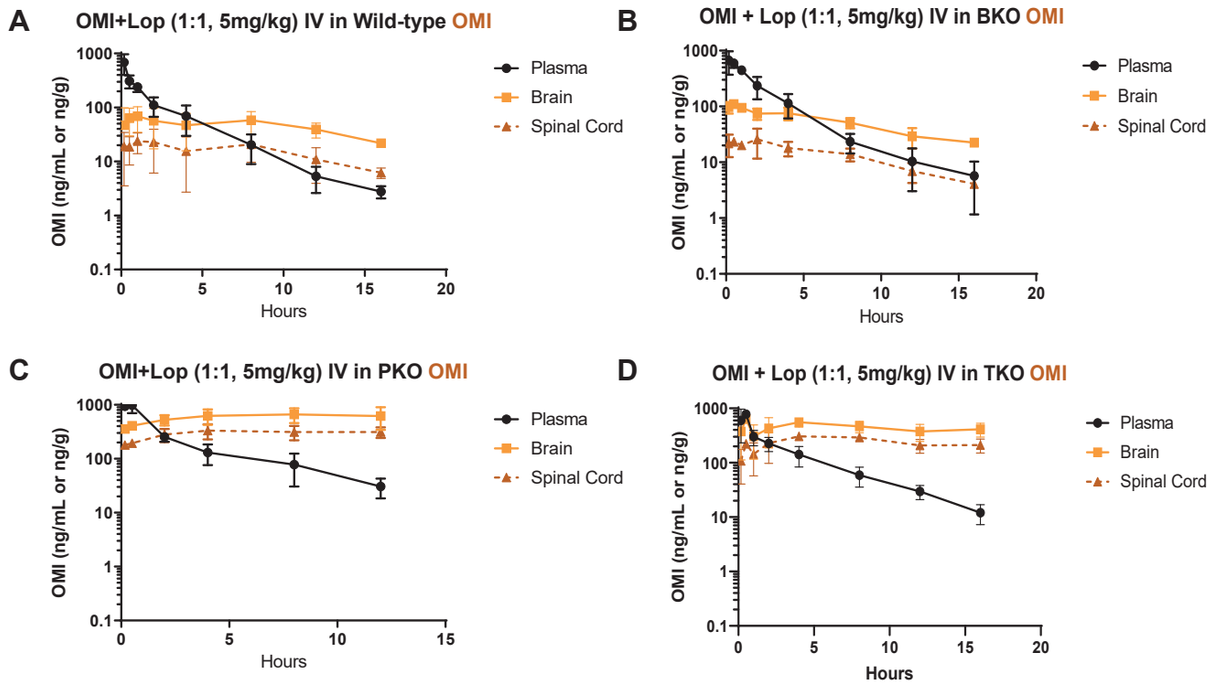

Supplementary Figure 4. OMI IV Pharmacokinetics and CNS Distribution when Co-administered with loperamide. Plasma, brain, and spinal cord concentration-time profiles following a single IV dose of OMI (5mg/kg) co-administered with loperamide (5mg/kg) in (A) Wild-type, (B) BCRP knockout, (C) P-gp knockout, and (D) triple knockout FVB mice